Calhoun
Institutional Archive of the Naval Postgraduate School

Calhoun: The NPS Institutional Archive

DSpace Repository

Theses and Dissertations 1. Thesis and Dissertation Collection, all items

1980

An analysis of LIDAR atmospheric remote sensing.

Hamon, Dale Robert

Monterey, California. Naval Postgraduate School

http://hdl.handle.net/10945/17520

This publication is a work of the U.S. Government as defined in Title 17, United States Code, Section 101. Copyright protection is not available for this work in the United States.

Downloaded from NPS Archive: Calhoun

DUDLEY KNOX LIBRARY

http://www.nps.edu/library

Calhoun is the Naval Postgraduate School's public access digital repository for research materials and institutional publications created by the NPS community. Calhoun is named for Professor of Mathematics Guy K. Calhoun, NPS's first appointed -- and published -- scholarly author.

Dudley Knox Library / Naval Postgraduate School
411 Dyer Road / 1 University Circle
Monterey, California USA 93943

DUDLEY KNOX LIBRARY
NAVAL POSTGRADUATE SCHOOL
MONTEREY, CALIF 93940

NAVAL POSTGRADUATE SCHOOL
Monterey, California

THESIS

AN ANALYSIS OF LIDAR
ATMOSPHERIC REMOTE SENSING

by

Dale Robert Hamon

June 1980

Thesis Advisor: E. C. Crittenden, Jr.

Approved for public release; distribution unlimited

T196289

REPORT DOCUMENTATION PAGE

READ INSTRUCTIONS
BEFORE COMPLETING FORM

1. REPORT NUMBER	2. GOVT ACCESSION NO.	3. RECIPIENT'S CATALOG NUMBER

4. TITLE (and Subtitle) AN ANALYSIS OF LIDAR ATMOSPHERIC REMOTE SENSING	5. TYPE OF REPORT & PERIOD COVERED Master's Thesis; June 1980 6. PERFORMING ORG. REPORT NUMBER
7. AUTHOR(s) Dale Robert Hamon	8. CONTRACT OR GRANT NUMBER(s)
9. PERFORMING ORGANIZATION NAME AND ADDRESS Naval Postgraduate School Monterey, California 93940	10. PROGRAM ELEMENT, PROJECT, TASK AREA & WORK UNIT NUMBERS
11. CONTROLLING OFFICE NAME AND ADDRESS Naval Postgraduate School Monterey, California 93940	12. REPORT DATE June 1980 13. NUMBER OF PAGES 101
14. MONITORING AGENCY NAME & ADDRESS(if different from Controlling Office)	15. SECURITY CLASS. (of this report) Unclassified 15a. DECLASSIFICATION/DOWNGRADING SCHEDULE

16. DISTRIBUTION STATEMENT (of this Report)

Approved for public release; distribution unlimited

17. DISTRIBUTION STATEMENT (of the abstract entered in Block 20, if different from Report)

Same as Block 16.

18. SUPPLEMENTARY NOTES

19. KEY WORDS (Continue on reverse side if necessary and identify by block number)

Mie Aerosol Distribution
LIDAR
Laser Radar

20. ABSTRACT (Continue on reverse side if necessary and identify by block number)

The analysis of scattered electromagnetic radiation is examined in terms of Mie theory establishing the detailed form for the scattering functions. These parameters are used to define the criterion whereby the composition and number densities of an atmospheric aerosol population may be assessed. Laser radar, or LIDAR, is the proposed remote sensing device and the governing system equations are developed. The problem of data inversion is surveyed with emphasis on smoothing methods, statistical analyses, and iterative techniques. A discussion of the numerical stability of the solution is also presented. On the basis of

20. the Mie model, inversion of the data provided by the LIDAR probe is given as a rationale to effect an estimate of the true particle number distribution function in an atmospheric cell.

Approved for public release; distribution unlimited

An Analysis of LIDAR
Atmospheric Remote Sensing

by

Dale Robert Hamon
Lieutenant, United States Navy
B.S., Auburn University, 1973

Submitted in partial fulfillment of the
requirements for the degree of

MASTER OF SCIENCE IN PHYSICS

from the

NAVAL POSTGRADUATE SCHOOL
June 1980

Thesis
H1756
c.1

DUDLEY KNOX LIBRARY
NAVAL POSTGRADUATE SCHOOL
MONTEREY, CALIF 93940

ABSTRACT

The analysis of scattered electromagnetic radiation is examined in terms of Mie theory establishing the detailed form for the scattering functions. These parameters are used to define the criterion whereby the composition and number densities of an atmospheric aerosol population may be assessed. Laser radar, or LIDAR, is the proposed remote sensing device and the governing system equations are developed. The problem of data inversion is surveyed with emphasis on smoothing methods, statistical analyses, and iterative techniques. A discussion of the numerical stability of the solution is also presented. On the basis of the Mie model, inversion of the data provided by the LIDAR probe is given as a rationale to effect an estimate of the true particle number distribution function in an atmospheric cell.

TABLE OF CONTENTS

I. INTRODUCTION ---------- 8

II. GENERAL SCATTERING THEORY ---------- 15

III. LIDAR ---------- 58

IV. MATHEMATICAL INVERSION ---------- 72

V. CONCLUSION ---------- 89

APPENDIX: COMPUTATIONAL FORMULAE AND ALGORITHM ---------- 91

COMPUTER (HP-41C) PROGRAM ---------- 97

LIST OF REFERENCES ---------- 99

INITIAL DISTRIBUTION LIST ---------- 101

LIST OF TABLES

TABLE I -- 10

TABLE II --- 61

TABLE III -- 75

LIST OF FIGURES

Figure 1 ---------- 9

Figure 2 ---------- 16

Figure 3 ---------- 17

Figure 4 ---------- 17

Figure 5 ---------- 22

Figure 6 ---------- 31

Figure 7 ---------- 35

Figure 8 ---------- 48

Figure 9 ---------- 62

Figure 10 ---------- 80

Figure 11 ---------- 95

Figure 12 ---------- 96

I. INTRODUCTION

The advent of sophisticated optical devices in both the scientific and defense communities has pointedly demonstrated the need to better understand the primary propagating and interacting medium characteristics of the earth's atmosphere. The intent of this paper is not to deal with the purpose of such devices, whether they are atmospheric pollutant monitors or infrared threat detectors. Rather the concern here is the use of these devices in the real world environment and the limitations imposed on them as a result of atmospheric optical signal degradation. This degradation is the result of manifold scattering effects such as Brillouin, Rayleigh, Mie, Fluorescent and Raman scattering and includes the atmospheric constituents' differential absorption of optical radiation. [2]

The atmospheric scattering and absorption centers include the air molecules, suspended particulates (aerosols) and water droplets in fog, rain or hail. The presence of aerosols strongly determines the transmission characteristics of the atmosphere and may even dominate the propagation characteristics. See Table I and figure 1 for a comparison of particle sizes and the range of number densities.

At the small end of the size spectrum are the air molecules themselves with radii of $10^{-4}\mu m$ and a concentration of 10^{19} per cm^3. The large end includes rain drops with radii of 10^2 to $10^4\mu m$ and a concentration of 10^{-5} to 10^{-2} per cm^3. The "small" particles, defined by a radius much less than the wavelength of radiation used as the probe,

Average size distribution of nuclei in
continental air masses

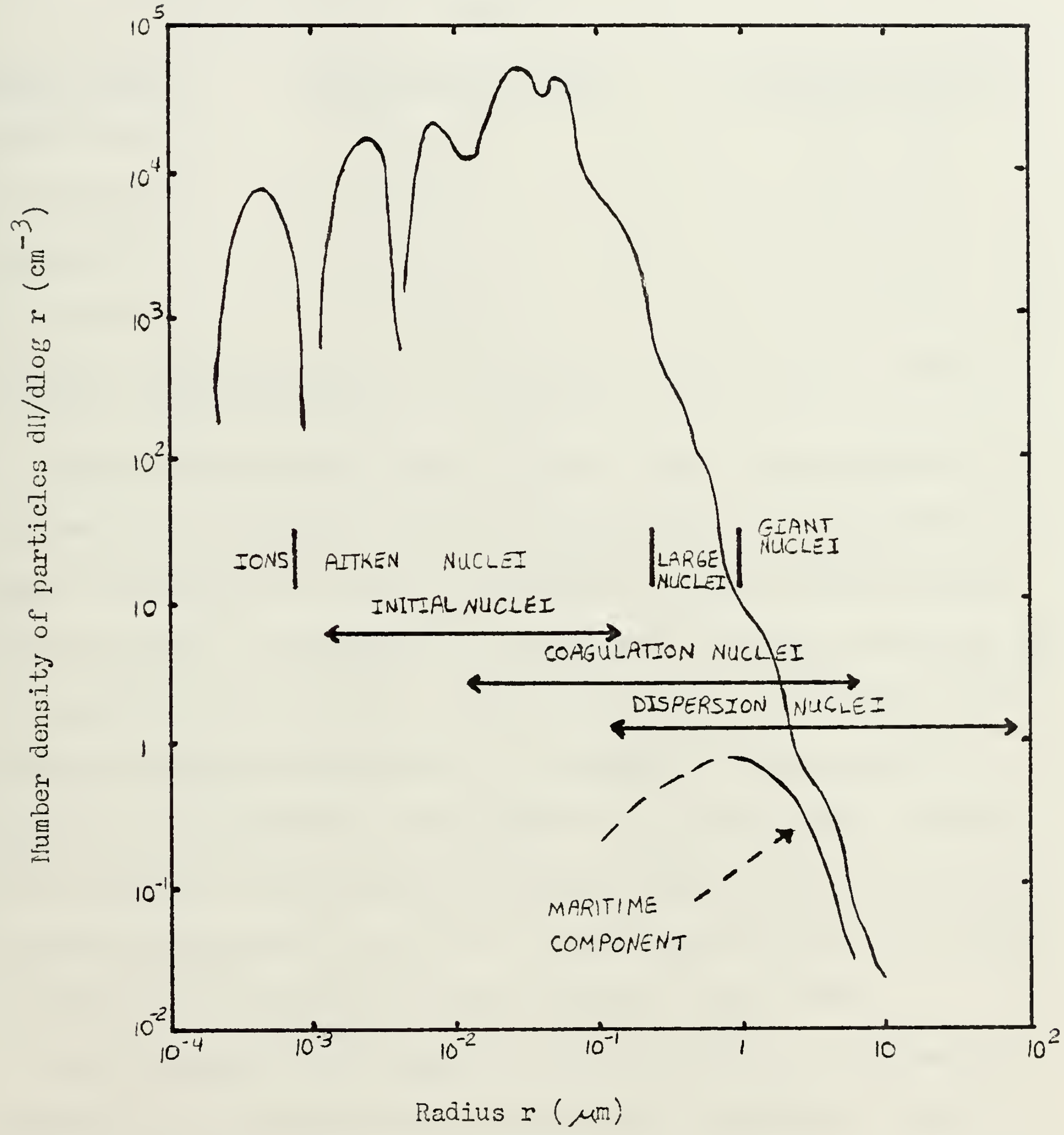

Figure 1 [6].

obey the Rayleigh scattering model, exhibiting a cross section that decreases proportionally as the particle radius to wavelength ratio to the fourth power. It is this fourth power law for molecular scattering that Rayleigh used to explain the blue color of the daytime sky.

TABLE I

Particle types	Particle Radius (μm)	Concentration (cm^{-3})
Aitken nuclei *	10^{-3} to 10^{-2}	10^{2} to 10^{4}
haze particles	10^{-2} to 1	10 to 10^{3}
fog droplets	1 to 10	10 to 10^{2}
cloud droplets	1 to 10	10 to 300

* Initial nuclei present in the atmosphere from the earth's surface [6] and/or meteoric sources.

For wavelengths larger than those of visible light, this scattering is very small. As the particle size approaches that of the radiation wavelength, the complete Mie theory is required to explain the scattering characteristics. The dependence on wavelength is highly oscillatory and very complex. As the particle grows still larger, its behavior in the radiation field approximates that of a large solid object casting a shadow field in proportion to its geometrical cross-section. The Mie theory includes both Rayleigh scattering for small radii and the "non-selective" scattering in the limit of large particle radii. The theory is covered in some detail in the next section of this paper.

Once one has both the atmospheric density and data on the aerosol composition and size distribution as functions of altitude, location, and time, the transmittance can be computed on a real-time basis by some rather sophisticated computer models.

Aerosols are colloidal particles dispersed and suspended or falling

slowly in the gaseous mixture of the atmosphere. Some examples are smokes, haze, clouds, small droplet (less than 1μm) fogs, and finely divided soils. These aerosols have as many sources as they have different forms and compositions. The chemical reaction of various atmospheric gasses whose minor components are nitrous oxides, terpenes, and hydrocarbons can produce solid particles. The presence of combustion products from inefficient burning, which may be locally critical, and, on a much larger scale, from forest fires and volcanic action serves only to increase the atmospheric load of particles that may take years to settle. Over large bodies of water, the dispersion of solutions into the near atmosphere region brings about the formation of fogs and rain as well as clouds. As a class, aerosols may either help or hinder the researcher. These particles may be used as tracers enhancing a received signal to detect atmospheric motions, distributions, and chemical composition. However, they primarily provide a large, random source of environmental noise. In this latter mode, the particle's presence tends to confuse the received signal at the sensor and provide noise that originates outside the system electronics, making it difficult, if not impossible, to supress. [6] Historically, aerosols have been divided into classes to facilitate their theoretical modeling. These models involve several free parameters that are designed to "best fit" the observed data. The classes are:

1. Maritime - This group is characterized primarily of sea salt with some water of hydration and a chlorine concentration slightly higher than sea water. Salt particle concentration decreases rapidly above a height of about 500 m.

2. Rural - The largest number of components are silicon, iron and some sulfates with approximately 10% to 15% organics. Of this total, about 1/3 of the aerosol is hygroscopic, whereby air moisture is readily absorbed. This same class is also found at sea at higher altitudes with a large particle density falling off rapidly as distance at sea increases.

3. Urban - Combustion products and the issue from industrial processes make up the bulk of this class.

4. Troposphere - This is an atmosphere division lying above the surface boundary layer and consists of the rural/maritime classes without large particles.

5. Stratosphere - Primarily (80% to 90%) consisting of the large sulfate ions and particulates, this group also shows a periodic large influx during volcanic activity.

The typical atmospheric analysis technique is to use two-ended systems requiring a source of radiation of known properties, a propagating path through the atmosphere of specific length and reasonably known conditions, and a stable receiver at the path's end. Experiments such as these are able to measure aerosol size and composition distributions to check out the various composition and scattering models. They also predict the performance characteristics of a particular optical device. However, two well-separated platforms are required with the attending problems of phasing and communications. Also, only low altitude, horizontal work can be done. A one-ended system would eliminate the need for one of the platforms and enable a full altitude/azimuthal capability in a real-time environment. There is a system that can easily be

adapted to the one-ended process and is available today. The laser radar, LIDAR, system is similar in operation to Radar with optical wavelengths instead of radio waves. In fact, the acronym is somewhat the same, meaning "Light Detection and Ranging". Conceptually, a laser pulse is emitted into the medium to be analyzed. This pulse interacts with the components of the medium and is both scattered and absorbed in distinct ways depending on the material type and density. Some portion of this pulse is returned as an echo to the point of origin where a telescope-like receiver is coupled to a photodetector that converts the received optical radiation into a proportional electrical signal. The pulse return timing is gated to the range of the atmospheric cell undergoing analysis. The intensity of the echo, the echo's polarization change, and any measured frequency shifts all undergo involved processing. The outputs can consist of composition, type, and size distributions. Some state of the art applications of the technique include: meterological LIDAR investigations; middle atmospheric LIDAR studies; tropospheric chemistry and diffusion research; studies of atmospheric propagation and radiative transfer; absorption, Raman and fluorescent spectroscopic applications; and pressure-temperature measurements of atmospheric layers. [2] A recent theoretical paper indicated that a series of measurements involving optical scattering and absorption can yield about 7 or 8 independent pieces of information concerning the aerosol size distribution within the analyzed cell, covering a range of particles with radii from $0.1\mu m$ to $5\mu m$. [20]

Consider such a single-ended LIDAR analysis system on board the type of mobile platform in use today by both scientific researchers and the

military. The optimum performance of a specific optical scanning/detection/tracking device could be evaluated in a real-time scenario without the need to resort to generalized models applicable only in standardized areas.

II. GENERAL SCATTERING THEORY

Scattering is the process whereby an incident electromagnetic wave loses energy and some portion of this energy undergoes re-emission. In general, the scattered wavefront has a different propagation direction than the incident wave. See figure 2.

For particles with a low number of electrons, the scattering can be computed using quantum mechanics. In this sense, the incident wave can only interact with the stationary states of the scattering particle's electronic system within a small bandwidth of frequencies about the allowed transition levels. One can discuss Rayleigh scattering as the absorption of the correct energy photon and the subsequent re-emission of a photon of essentially the same energy. An energy level diagram would look like figure 3.

Likewise, Raman scattering involves a definite frequency shift between the incident and scattered radiation. If the scattered frequency is less than that of the incident, the process produces the Stokes lines spectroscopically. And when the reverse is true, the anti-Stokes condition exists. [8] See figure 4.

However, for molecular and larger particle scattering, the collection of electronic states becomes great enough to let us deal with the problem classically. The particle is considered to be a solid dielectric with a complex index of refraction.

One of the most widely studied problems in diffraction theory is electromagnetic and acoustic wave scattering by a sphere. The problem of diffraction of a plane-monochromatic wave by a homogeneous sphere

Scattering of a plane wave off a small particle

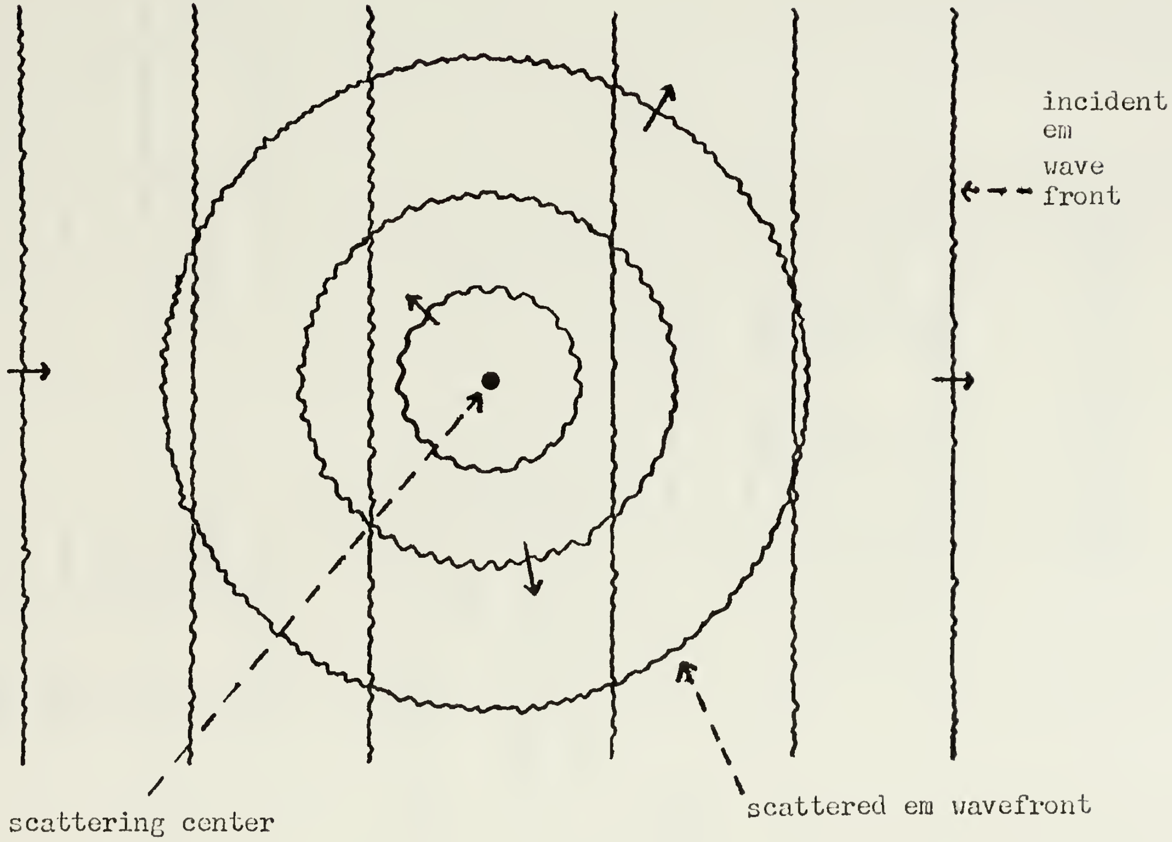

Figure 2

Atomic level scattering

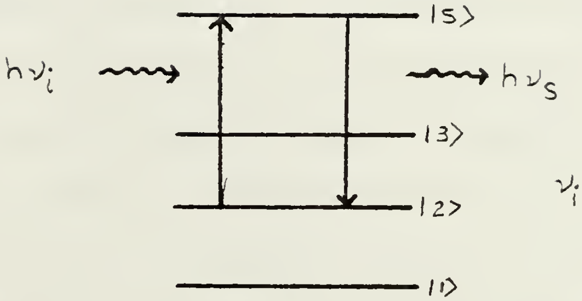

$\nu_i = \nu_s$

Figure 3

$h\nu_i$: incident photon energy

$h\nu_s$: scattered photon energy

$|1,2,3\rangle$: state levels

$|s\rangle$: intermediate stable/unstable state

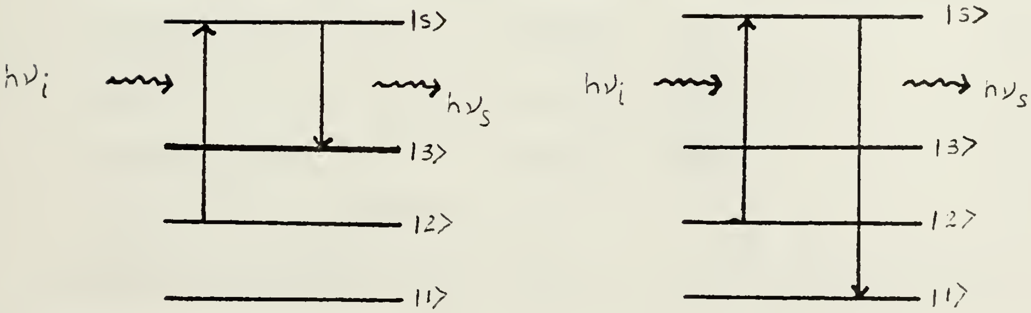

$\nu_i > \nu_s$: Stokes

$\nu_i < \nu_s$: anti-Stokes

Figure 4

characterized by its radius and complex index of refraction was rigorously solved by G. Mie in 1908. His analysis involved the solving of Maxwell's equations for the electromagnetic field when an incident plane wave interacts with a material interface. When the discrete boundary separates media of different optical characteristics, a scattered wave is generated.

Today, an extensive bibliography of approaches to this problem exists. The author will follow the analysis presented by Kerker (1969) [12] throughout this section in order to present a consistent derivation. First, the salient features of the Maxwell theory will be listed, leading to the wave equation. The solution satisfying the appropriate boundary conditions will be obtained; the resulting infinite series solution not only completely defines the scattered wave, but gives the electromagnetic states of the particules' interior as well. The single particle scattering results will be compiled and extended to cover collective scattering.

Maxwell's equations, in rationalized MKS units: [12], [15]

Coulomb's law $\nabla \cdot \underset{\sim}{D} = \rho$ (1)

Ampere's law $\nabla \times \underset{\sim}{H} = \frac{\partial}{\partial t}\underset{\sim}{D} + \underset{\sim}{J}$ (2)

Faraday's law $\nabla \times \underset{\sim}{E} = \frac{-\partial}{\partial t}\underset{\sim}{B}$ (3)

absence of free magnetic poles $\nabla \cdot \underset{\sim}{B} = 0$ (4)

The symbol $\underset{\sim}{V}$ denotes a vector quantity. Following are definitions of vectors used in derivation:

$\underset{\sim}{E}$ - electric field intensity (volts/meter)

$\underset{\sim}{H}$ - magnetic field intensity (amps/meter)

$\underset{\sim}{D}$ - electric flux density (dielectric displacement, coulomb/meter^2)

$\underset{\sim}{B}$ - magnetic flux density (magnetic induction, weber/meter^2)

$\underset{\sim}{J}$ - electric current density (amps/meter^2)

ρ - electric charge density (coulomb/meter^3)

t - time (seconds)

These equations will define the electromagnetic field configuration for all points in space and uniquely determine the field vectors given the media characteristics below.

$$\underset{\sim}{D} = \varepsilon \underset{\sim}{E} \tag{5}$$

$$\underset{\sim}{B} = \mu \underset{\sim}{H} \tag{6}$$

$$\underset{\sim}{J} = \sigma \underset{\sim}{E} \tag{7}$$

The media parameters thus defined are:

ε - permittivity (electric inductive capacity, farads/meter)

μ - permeability (magnetic inductive capacity, henrys/meter)

σ - conductivity (specific conductance, 1/ohm-meter)

In free space (vacuo):

$\varepsilon = \varepsilon_0 = 8.8542 \times 10^{-12}$ farad/m

$\mu = \mu_0 = 4\pi \times 10^{-7}$ henry/m

As a consequence of the invariance of the Maxwell equations, the quantity $(\mu\varepsilon)^{-\frac{1}{2}}$ has the units of velocity and, again, in free space:

$$C = (\mu_0\varepsilon_0)^{-1/2} = 2.997925 \times 10^8 \text{ m/sec} \tag{8}$$

This last quantity is the speed of light in vacuum. When the quantities $\varepsilon, \mu,$ and σ are independent of direction, the region in space they characterize is said to be isotropic. Two more equations are required to complete the picture.

Lorentz Force $\underset{\sim}{F} = \rho(\underset{\sim}{E} + \underset{\sim}{u} \times \underset{\sim}{B})$ (9)

Newton's second law of motion $\underset{\sim}{F} = m\underset{\sim}{a}$ (10)

Where: $\underset{\sim}{F}$ - force on charged particle (newtons)

$\underset{\sim}{u}$ - velocity of charged particle (m/s)

$\underset{\sim}{m}$ - mass of charged particle (kg)

$\underset{\sim}{a}$ - acceleration of charged particle (m/s^2)

All macroscopic, linear, electromagnetic phenomenon are described by equations (1) through (10) with the associated quantity definitions. The classical dynamics of interacting charged particles and electromagnetic fields are thus specified.

A certain degree of convenience is obtained using the definitions of the two following auxillary vectors:

$$\underset{\sim}{P} = \underset{\sim}{D} - \varepsilon_o \underset{\sim}{E} \tag{11}$$

$$\underset{\sim}{M} = (1/\mu_o)\underset{\sim}{B} - \underset{\sim}{H} \tag{12}$$

Where: $\underset{\sim}{P}$ - electric polarization (c/m^2)

$\underset{\sim}{M}$ - magnetic polarization (A/m)

One can see that, in free space, these quantities vanish identically and they may then be considered as a measure of the effect of matter on the local fields. Some dimensionless quantities may also be defined:

$$K_e = \varepsilon/\varepsilon_o \tag{13}$$

$$K_m = \mu/\mu_o \tag{14}$$

Where: K_e - specific ε (relative dielectric constant)

K_m - specific μ (relative magnetic permeability)

The media may further be described with:

$$\underset{\sim}{P} = \chi_e \varepsilon_o \underset{\sim}{E} \tag{15}$$

$$\underset{\sim}{M} = \chi_m \underset{\sim}{H} \tag{16}$$

Where: χ_e - electric susceptibility

χ_m - magnetic susceptibility

The previous set of equations can be combined to obtain:

$$\chi_e = K_e - 1 \tag{17}$$

$$\chi_m = K_m - 1 \tag{18}$$

Maxwell's equations apply to regions where the media may be represented by the continuous functions $\varepsilon, \mu,$ and σ. When a medium discontinuity is encountered, such as the conditions across a regional interface, the fields must satisfy a specific set of relations at the boundary. See figure 5. Let:

$\underset{\sim}{J}_S$ - surface current density on interface S (A/m^2)

ρ_s - surface charge density on interface S (c/m^2)

The Maxwell equations (1) - (4) are cast in point form for each differential point in space. One can apply various integral theorems to change the same equations to integral form and use them to define the conditions that the fields must satisfy by crossing the interface. [17] The boundary conditions obtained are inherent in the Maxwell equations.

Boundary conditions:

(a) the tangential component of $\underset{\sim}{E}$ is continuous

$$(\underset{\sim}{E}_2 - \underset{\sim}{E}_1) \times \underset{\sim}{n} = 0 \tag{19}$$

(b) The tangential component of $\underset{\sim}{H}$ undergoes a discontinuity equal to $\underset{\sim}{J}_s$

$$(\underset{\sim}{H}_2 - \underset{\sim}{H}_1) \times \underset{\sim}{n} = \underset{\sim}{J}_s \tag{20}$$

(c) The normal component of $\underset{\sim}{D}$ undergoes a discontinuity equal to ρ_s

$$(\underset{\sim}{D}_2 - \underset{\sim}{D}_1) \cdot \underset{\sim}{n} = \rho_s \tag{21}$$

(d) the normal component of $\underset{\sim}{B}$ is continuous

$$(\underset{\sim}{B}_2 - \underset{\sim}{B}_1) \cdot \underset{\sim}{n} = 0 \tag{22}$$

For all cases of dielectric scattering, it is assumed that there is no free surface charge or current density. This assumption begins to break down for large particles in the presence of storm activity. However, we

Media optical boundary

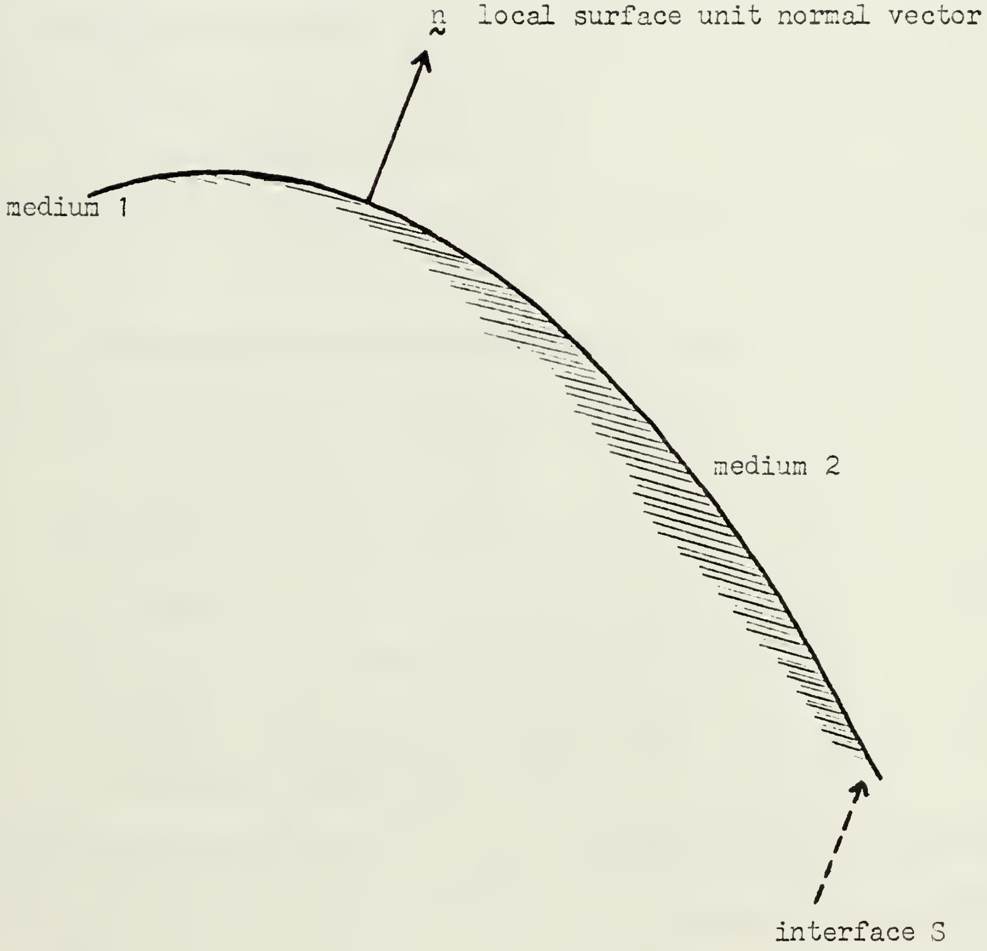

Figure 5

will, for simplicity, assume that $\underset{\sim}{J}_s = \underset{\sim}{0}$ and $\rho_s = 0$. Therefore, the tangential components of $\underset{\sim}{E}$ and $\underset{\sim}{H}$ and the normal components of $\underset{\sim}{D}$ and $\underset{\sim}{B}$ are continuous across the boundary.

Charge conservation is included in the Maxwell theory and is written as:

$$\text{continuity equation} \quad \nabla \cdot \underset{\sim}{J}_v + \frac{\partial}{\partial t}\rho_v = 0 \tag{23}$$

Where: $\underset{\sim}{J}_v$ - volume current density (A/m^3)

ρ_v - volume charge density (c/m^3)

Throughout the following derivation, a few vector identities will be required.

Note: $\underset{\sim}{A}$ - continuously differentiable vector field

ϕ - continuously differentiable scalar field

$$\left.\begin{aligned}
&\nabla \cdot (\nabla \times \underset{\sim}{A}) = 0 \\
&\nabla \cdot (\nabla \phi) = \nabla^2 \phi \\
&\nabla \times (\nabla \phi) = 0 \\
&\nabla \cdot (\phi \underset{\sim}{A}) = \underset{\sim}{A} \cdot (\nabla \phi) + \phi (\nabla \cdot \underset{\sim}{A}) \\
&\nabla \times (\phi \underset{\sim}{A}) = \phi (\nabla \times \underset{\sim}{A}) + (\nabla \phi) \times \underset{\sim}{A} \\
&\nabla \times (\nabla \times \underset{\sim}{A}) = \nabla (\nabla \cdot \underset{\sim}{A}) - \nabla^2 \underset{\sim}{A}
\end{aligned}\right\} \tag{24}$$

If the fields described by (1) - (4) are invariant under a gauge transformation, then they are well defined by the preceding formalism.[16]

We define:

$\underset{\sim}{A}$ - vector potential field

ϕ - scalar potential field

in the following relations.

$$\underset{\sim}{B} = \nabla \times \underset{\sim}{A} \tag{25}$$

Compare this to equations (4) and (24). Using equation (25) in (3), we

get the following:

$$\nabla \times \underset{\sim}{E} = -\frac{\partial}{\partial t}(\nabla \times \underset{\sim}{A}) = -\nabla \times \left(\frac{\partial}{\partial t}\underset{\sim}{A}\right)$$

$$\Rightarrow \nabla \times \left(\underset{\sim}{E} + \frac{\partial}{\partial t}\underset{\sim}{A}\right) = 0$$

Now, refering to (24),

$$\Rightarrow \underset{\sim}{E} + \frac{\partial}{\partial t}\underset{\sim}{A} = -\nabla \phi$$,thus

$$\underset{\sim}{E} = \frac{\partial}{\partial t}\underset{\sim}{A} - \nabla \phi \tag{26}$$

A and ϕ are not unique. Let g be any scalar function, then the new potential can be defined as:

$$\underset{\sim}{A}' = \underset{\sim}{A} - \nabla g \tag{27}$$

$$\phi' = \phi + \frac{\partial}{\partial t} g \tag{28}$$

Now the fields $\underset{\sim}{E}$ and $\underset{\sim}{B}$ are recomputed.

$$\underset{\sim}{B}' = \nabla \times (\underset{\sim}{A} - \nabla g) = \underset{\sim}{B} - \nabla \times (\nabla g) = \underset{\sim}{B}$$

$$\Rightarrow \quad \underset{\sim}{B}' = \underset{\sim}{B}$$

$$\underset{\sim}{E}' = -\frac{\partial}{\partial t}(\underset{\sim}{A} - \nabla g) - \nabla\left(\phi + \frac{\partial}{\partial t} g\right) = -\frac{\partial}{\partial t}\underset{\sim}{A} - \nabla \phi + \frac{\partial}{\partial t}(\nabla g) - \nabla \frac{(\partial g)}{\partial t}$$

$$\Rightarrow \quad \underset{\sim}{E}' = \underset{\sim}{E}$$

The physical observables are the fields $\underset{\sim}{E}$ and $\underset{\sim}{B}$ and it can be seen that the gauge transformation defined by (27) and (28) leaves these fields unchanged. Thus, the Maxwell equations are gauge invariant.

We now turn from formalism to a more practical aspect of electromagnetic theory and introduce the Wave Equation:

$$\nabla \times (3): \nabla \times (\nabla \times \underset{\sim}{E}) = \frac{-\partial}{\partial t}(\nabla \times \underset{\sim}{B})$$

Note that the time and space operations of differentiation are commutative for these continuously differentiable functions.

$$(6), (24): \nabla (\nabla \cdot \underset{\sim}{E}) - \nabla^2 \underset{\sim}{E} = -\frac{\partial}{\partial t}(\nabla \times \mu \underset{\sim}{H})$$

The assumption is always made that all space and time derivations of the parameters ε, μ, and σ are either slowly varying with respect to the rate

of change of the fields themselves or identically equal to zero.

$$\Rightarrow \nabla(\nabla\cdot\underset{\sim}{E}) - \nabla^2\underset{\sim}{E} = -\mu\frac{\partial}{\partial t}(\nabla\times\underset{\sim}{H})$$

$$(1),\ (2),\ (5),\ (7):\ \nabla\cdot(\varepsilon\underset{\sim}{E}) = \varepsilon\nabla\cdot\underset{\sim}{E} = \rho$$

$$\Rightarrow \nabla\cdot\underset{\sim}{E} = \rho/\varepsilon$$

$$\nabla\times\underset{\sim}{H} = \frac{\partial}{\partial t}(\varepsilon\underset{\sim}{E}) + \sigma\underset{\sim}{E} = \varepsilon\frac{\partial}{\partial t}\underset{\sim}{E} + \sigma\underset{\sim}{E}$$

$$\Rightarrow \nabla\times\underset{\sim}{H} = \sigma\underset{\sim}{E} + \varepsilon\frac{\partial}{\partial t}\underset{\sim}{E}$$

$$\Rightarrow \nabla(\rho/\varepsilon) - \nabla^2\underset{\sim}{E} = -\mu\frac{\partial}{\partial t}\left(\sigma\underset{\sim}{E} + \varepsilon\frac{\partial}{\partial t}\underset{\sim}{E}\right)$$

The same argument also applies to the quantity ρ/ε concerning its rate of change with the rate of change of the fields.

$$\Rightarrow \nabla^2\underset{\sim}{E} = \sigma\mu\frac{\partial}{\partial t}\underset{\sim}{E} + \varepsilon\mu\frac{\partial^2}{\partial t^2}\underset{\sim}{E}$$

Therefore: $$\nabla^2\underset{\sim}{E} - \sigma\mu\frac{\partial}{\partial t}\underset{\sim}{E} - \varepsilon\mu\frac{\partial^2}{\partial t^2}\underset{\sim}{E} = 0 \tag{29}$$

This equation, (29), is the well-known nonhomogeneous equation for damped wave motion - the Wave Equation. Similarly, ∇ X (2):

$$\nabla\times(\nabla\times\underset{\sim}{H}) = \frac{\partial}{\partial t}(\nabla\times\underset{\sim}{D}) + (\nabla\times\underset{\sim}{J})$$

$$(5),\ (7),\ (24):\ \nabla(\nabla\cdot\underset{\sim}{H}) - \nabla^2\underset{\sim}{H} = \varepsilon\frac{\partial}{\partial t}(\nabla\times\underset{\sim}{E}) + \sigma(\nabla\times\underset{\sim}{E})$$

$$(4) \Rightarrow \nabla\cdot(\mu\underset{\sim}{H}) = \mu\nabla\cdot\underset{\sim}{H} = 0 \Rightarrow \nabla\cdot\underset{\sim}{H} = 0$$

$$(3):\ -\nabla^2\underset{\sim}{H} = \varepsilon\frac{\partial}{\partial t}\left(\frac{-\partial\underset{\sim}{B}}{\partial t}\right) + \sigma\left(\frac{-\partial\underset{\sim}{B}}{\partial t}\right)$$

$$(6):\ -\nabla^2\underset{\sim}{H} = -\varepsilon\mu\frac{\partial^2}{\partial t^2}\underset{\sim}{H} - \sigma\mu\frac{\partial}{\partial t}\underset{\sim}{H}$$

$$\Rightarrow \nabla^2\underset{\sim}{H} - \sigma\mu\frac{\partial}{\partial t}\underset{\sim}{H} - \varepsilon\mu\frac{\partial^2}{\partial t^2}\underset{\sim}{H} = 0 \tag{30}$$

The relations for non-dissipative media are obtained by setting $\sigma = 0$. Both equations (29) and (30) actually represent 3 equations each. Each component of the vector field must satisfy these equations for the vector field itself to do so. Let the symbol u correspond to any of the six components of the two fields $\underset{\sim}{E}$ and $\underset{\sim}{H}$. The scalar wave equation can be expressed by:

$$\nabla^2 u - \sigma\mu\frac{\partial u}{\partial t} - \varepsilon\mu\frac{\partial^2 u}{\partial t^2} = 0 \tag{31}$$

The fields described by (31) represent a transfer of energy in both space and time. The electromagnetic wave has a time periodicity that suggests a form for the energy flux crossing a unit area per unit time:

$$\underset{\sim}{S} = \underset{\sim}{E} \times \underset{\sim}{H} \tag{32}$$

Equation (32) is the Poynting vector equation, whose time averaged magnitude over the period of the wave yields the wave intensity,

$$I = 1/\tau \int_0^{\tau} |\underset{\sim}{S}| \, dt \tag{33}$$

where τ is the period of the wave. The field symbols $\underset{\sim}{E}$ and $\underset{\sim}{H}$ in (32) are the real parts of the complex fields whose components satisfy (31).

The form of the scalar wave equation suggests a harmonic time dependence of the form:

$$U(\underset{\sim}{r},t) = f(\underset{\sim}{r})e^{i\omega t} \tag{34}$$

where ω is the angular frequency, $i = \sqrt{(-1)}$, and $\underset{\sim}{r}$ is the usual three-dimensional position vector. Note that:

$$\frac{\partial U}{\partial t} = i\omega U \qquad \text{and} \qquad \frac{\partial^2 U}{\partial t^2} = -\omega^2 U$$

then, (31): $\nabla^2 U - \sigma\mu i\omega U + \varepsilon\mu\omega^2 U = 0$

$$\Rightarrow \nabla^2 U + (\mu\varepsilon\omega^2 - i\mu\sigma\omega)U = 0$$

Define the propagation constant k by:

$$K^2 = \mu\varepsilon\omega^2 - i\mu\sigma\omega \tag{35}$$

then: $$\nabla^2 U + K^2 U = 0 \tag{36}$$

Equation (36) is the Helmholtz Wave Equation. Another form of (35) is:

$$K = \alpha_1 - i\beta_1 \tag{37}$$

where: $$\alpha_1 = \omega\left\{\frac{\mu\varepsilon}{2}\left[\left(1+\frac{\sigma^2}{\varepsilon^2\omega^2}\right)^{1/2} + 1\right]\right\}^{1/2} \tag{38}$$

$$\beta_1 = \omega\left\{\frac{\mu\varepsilon}{2}\left[\left(1+\frac{\sigma^2}{\varepsilon^2\omega^2}\right)^{1/2} - 1\right]\right\}^{1/2} \tag{39}$$

It is the β_1 term that determines the damping undergone by the wave per unit path length; the energy is dissipated as Joule heat in the medium

when $\sigma > 0$.

Recalling that the quantity

$$V = (\mu \varepsilon)^{1/2} \tag{40}$$

is a velocity which, in free space is c, the relation for an electromagnetic wave in a medium described by light speed V is

$$\lambda \nu = V \tag{41}$$

where: λ - wavelength

ν - frequency

V - velocity of the wave

Also,

$$2\pi\nu = \omega \tag{42}$$

and this is the angular frequency, ω, mentioned earlier. In free space,

$$\lambda_0 \nu = c \tag{43}$$

The index of refraction, n, is defined as

$$n = c/V \tag{44}$$

(41), (43), (44): $n = \dfrac{\lambda_0 \nu}{\lambda \nu} = \lambda_0/\lambda$

$$\Rightarrow \quad n\lambda = \lambda_0 \tag{45}$$

It is clear that λ_0 is the wavelength when the wave is propagated in free space. In the same medium, $\sigma = 0$ implies that

$$\beta_1 = 0 \quad \Rightarrow \alpha_1 = \omega(\mu_0 \varepsilon_0)^{1/2} = \omega/c$$

$$\Rightarrow \quad K_0 = \omega/c = 2\pi\nu/\lambda_0\nu$$

$$\Rightarrow \quad K_0 = 2\pi/\lambda_0 \tag{46}$$

This k_0 is the free space propagation constant.

The complex refractive index, m, can be defined as

$$m = K/K_0 = n(1 - i\kappa) \tag{47}$$

where: κ - index of absorption (extinction)

As an example, suppose that there is a plane wave propagating along the

z - axis whose x - component is:

$$E_x = Ae^{i(\omega t - Kz)}$$

$$(47):\ E_x = Ae^{i\omega t}e^{-imK_o z} = Ae^{i\omega t}e^{-inK_o(1-iX)z}$$

$$\Rightarrow E_x = Ae^{i\omega t}e^{-inK_o z}e^{-nK_o Xz}$$

$$\Rightarrow E_x = Ae^{i(\omega t - nK_o z)}e^{-nK_o Xz}$$

The attenuation of the wave is seen explicitly as $e^{-nk_o Xz}$. An expansion of this example shows that the resultant plane wave solution leads directly to the Stokes parameters. Assume the propagation direction is z, as stated earlier, and that the monochromatic wave is traveling unbound in a source free isotropic medium. It is assumed that the wave can by completely specified in the xy-plane by the z,t coordinates of the wave. Thus:

$$\nabla^2 u = \frac{\partial^2 u}{\partial z^2}(z,t) \quad \Rightarrow \quad \frac{\partial u}{\partial x} = \frac{\partial u}{\partial y} = 0$$

$$(34),\ (36):\ \left[\frac{d^2 f(z)}{dz^2} + K^2 f(z)\right]e^{i\omega t} = 0$$

$$\frac{d^2 f}{dz^2} + K^2 f = 0$$

Substituting a trial solution, $f = ae^{bz}$,

$$\Rightarrow ab^2e^{bz} + K^2ae^{bz} = 0 \quad \Rightarrow b^2 = -k^2,\ b = \pm ik$$

$$\Rightarrow f(z) = ae^{\pm iKz}$$

From the definition of k, -ikz is selected as the value.

$$\Rightarrow U(z,t) = ae^{i(\omega t - Kz)}$$

This equation describes the form for each of the six vector components of $\underset{\sim}{E}$ and $\underset{\sim}{H}$. Recalling (1), under the present constraints:

$$(1)\quad \frac{\partial E_x}{\partial x} + \frac{\partial E_y}{\partial y} + \frac{\partial E_z}{\partial z} = 0 \qquad \text{and } U = E_x, E_y, \text{ and } E_z.$$

But, $\frac{\partial u}{\partial x} = \frac{\partial u}{\partial y} = 0 \Rightarrow \frac{\partial E_z}{\partial z} = 0 \Rightarrow E_z = 0$

$$\Rightarrow E_x = a_x^E e^{i(\omega t - kz)} \quad \text{and} \quad E_y = a_y^E e^{i(\omega t - kz)}$$

(3), (6) $\nabla \times \underset{\sim}{E} = -\mu\frac{\partial H}{\partial t} \Rightarrow -\mu\frac{\partial H}{\partial t}x = \frac{-\partial E}{\partial z}y$,

$$\Rightarrow -\mu\frac{\partial H}{\partial t}y = \frac{\partial E}{\partial z}x \quad , \quad -\mu\frac{\partial H}{\partial t}z = 0 \quad \Rightarrow \quad H_z = 0$$

It is quite sufficient to describe the behavior of $\underset{\sim}{E}$ as the value of $\underset{\sim}{H}$ can be readily obtained using equations (1) through (4). Given the form of u(z,t):

$$\frac{\partial H}{\partial t}x = i\omega H_z \quad , \quad \frac{\partial H}{\partial t}y = i\omega H_y$$

$$\frac{\partial E}{\partial z}x = -ikE_x \quad , \quad \frac{\partial E}{\partial z}y = -ikE_y$$

$$\Rightarrow -\mu i\omega H_x = +ikE_y \Rightarrow H_x = \frac{-k}{\mu\omega}E_y$$

$$\Rightarrow -\mu i\omega H_y = -ikE_x \Rightarrow H_y = \frac{k}{\mu\omega}E_x$$

Note: $E_x/H_y = -E_y/H_x = \mu\omega/k$

The term $\mu\omega/k$ can be reduced using (35) to the following:

$$\frac{\mu\omega}{k} = \mu\omega\left[\mu\omega^2(\varepsilon - i\sigma/\omega)\right]^{-1/2} \Rightarrow \frac{\mu\omega}{k} = \frac{\mu\omega}{\mu\omega}\left(\frac{\mu}{\varepsilon - \frac{i\sigma}{\omega}}\right)^{1/2}$$

Defining the intrinsic impedance of the medium for plane waves as

$$Z_o = \left(\frac{\mu}{\varepsilon - \frac{i\sigma}{\omega}}\right)^{1/2} \qquad (48)$$

$$\Rightarrow \frac{E_x}{H_y} = \frac{-E_y}{H_x} = Z_o$$

Finally, $\underset{\sim}{E}$ for the plane wave is:

$$\left.\begin{aligned} E_x &= Ae^{i(\omega t - kz + \delta_1)} \\ E_y &= Be^{i(\omega t - kz + \delta_2)} \\ E_z &= 0 \end{aligned}\right\} \qquad (49)$$

where δ_1 and δ_2 are arbitrary phase angles to account for the general history of the wave. The H wave is also determined by equation (49):

$$\left.\begin{aligned} H_x &= -\frac{1}{Z_o}Be^{i(\omega t - kz + \delta_2)} \\ H_y &= \frac{1}{Z_o}Ae^{i(\omega t - kz + \delta_1)} \\ H_z &= 0 \end{aligned}\right\} \qquad (50)$$

We see that:

$$\underset{\sim}{E}\cdot\underset{\sim}{H} = E_xH_x + E_yH_y = \frac{-E_xE_y}{Z_o} + \frac{E_yE_x}{Z_o} = 0$$

$$\Rightarrow \quad \underset{\sim}{E}\cdot\underset{\sim}{H} = 0 \tag{51}$$

Thus, $\underset{\sim}{E}$ and $\underset{\sim}{H}$ are perpendicular to each other for the plane wave solution.

The concept of polarized light can now be introduced with the help of equation (49), δ_1, and δ_2. The general plane wave solution describes an elliptical rotation of the $\underset{\sim}{E}$ vector in the plane perpendicular to the direction of propagation. Defining the phase difference as δ:

$$\delta = \delta_2 - \delta_1 \tag{52}$$

The representation of the state of a polarized wave can then be uniquely determined using the Stokes parameters, which are:

$$S_0 = A^2 + B^2 = A_1^2 + B_1^2 \tag{53}$$

$$S_1 = A^2 - B^2 = S_0 \cos 2\Psi \cos 2\chi \tag{54}$$

$$S_2 = 2AB\cos\delta = S_0 \sin 2\Psi \cos 2\chi \tag{55}$$

$$S_3 = 2AB\sin\delta = S_0 \sin 2\chi \tag{56}$$

The lengths A_1 and B_1 and the angles Ψ, and χ are illustrated in figure 6.

The quantity (ωt - kz) can be eliminated from (49) using equation (52), where E_x and E_y refer to the real parts of the complex wave:

$$\left(\frac{E_x}{A}\right)^2 + \left(\frac{E_y}{B}\right)^2 - \frac{2E_xE_y}{AB}\cos\delta = \sin^2\delta \tag{57}$$

This is the equation of an ellipse. The ellipse in figure 6 is drawn "right-handed", that is, the head of the electric field vector follows the arrows when viewing the wavefront face on. In order to exhibit right-handed polarization, $\sin\delta > 0$ and $0 < \chi \leq \pi/4$. Linear polarization exists when:

$$\delta = j\pi, \quad j = 0, \pm 1, \pm 2, \pm 3, \ldots \tag{58}$$

and circular polarization corresponds to

$$\delta = \tfrac{1}{2} j\pi, \quad j = \pm 1, \pm 3, \pm 5, \pm 7, \ldots \tag{59}$$

Pictorial definition of the
quantities A_1, B_1, ψ, χ

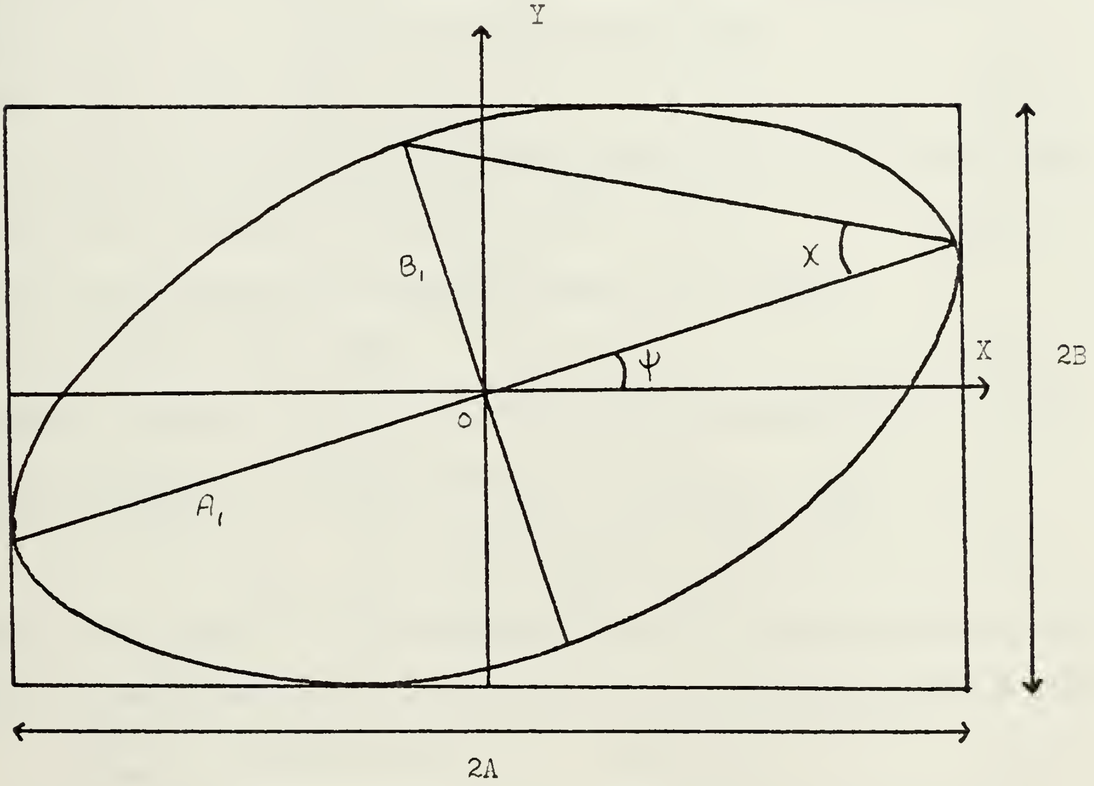

$\tan \chi = \pm B_1/A_1$ $\quad (-\pi/4 \leq \chi \leq \pi/4)$, $(0 \leq \psi < \pi)$

Figure 6

The Stokes parameters satisfy:

$$S_0^2 = S_1^2 + S_2^2 + S_3^2 \tag{60}$$

and a complete state of polarization is obtained from only three independent parameters.

Natural light is defined as the state where the intensity of light is the same in any direction perpendicular to the propagation vector, $\underset{\sim}{k}$. The phases of the various components in natural light are randomly varying so that no correlation exists between them.

$$\Rightarrow \quad S_1^n = S_2^n = S_3^n = 0 \tag{61}$$

The combination of elliptically polarized beams can be accomplished using:

$$S_0 = \sum_i S_{0i}\,, \quad S_1 = \sum_i S_{1i}\,, \quad S_2 = \sum_i S_{2i}\,, \quad S_3 = \sum_i S_{3i} \tag{62}$$

Then for non-identical polarization states for all beams:

$$S_0^2 > S_1^2 + S_2^2 + S_3^2 \tag{63}$$

Partially polarized light can be described as a superposition of natural light and a set of incoherent beams:

$$S_0 = S_0^n + S_0^p\,, \quad S_1 = S_1^p\,, \quad S_2 = S_2^p\,, \quad S_3 = S_3^p\,, \quad \text{and} \quad S_0^p = \left(S_1^2 + S_2^2 + S_3^2\right)^{1/2} \tag{64}$$

Finally, the fraction of polarization, F, can be defined as the intensity ratio of the polarized part of the wave to the total wave superposition:

$$F = \frac{I_{pol}}{I_{tot}} = S_0^p/(S_0^n + S_0^p) \qquad (0 \leq F \leq 1) \tag{65}$$

It can be shown that the parameters of a scattered wave are linearly dependent on the parameters of the incident wave. [10] This relation is written as follows:

$$I_s = (1/R^2)\, \underset{\sim}{\bar{\sigma}}\, I_i \tag{66}$$

where: R - observation distance to scatterer

i - incident wave

s - scattered wave

$$I = \begin{pmatrix} I_1 \\ I_2 \\ U \\ V \end{pmatrix}$$

The modified Stokes parameters are defined first by writing equation (49) as:

$$E_x = E_1 e^{i\omega t} \quad , \quad E_y = E_2 e^{i\omega t} \tag{67}$$

then,

$$I_1 = |E_1|^2 \tag{68}$$

$$I_2 = |E_2|^2 \tag{69}$$

$$U = 2 \operatorname{Re} \{E_1 E_2{}^*\} \tag{70}$$

$$V = 2 \operatorname{Im} \{E_1 E_2{}^*\} \tag{71}$$

The 4X4 Stokes matrix $\underset{\sim}{\bar{\sigma}}$ looks like this:

$$\underset{\sim}{\bar{\sigma}} = \begin{pmatrix} |f_{11}|^2 & |f_{12}|^2 & \operatorname{Re}(f_{11} f_{12}^*) & -\operatorname{Im}(f_{11} f_{12}^*) \\ |f_{21}|^2 & |f_{22}|^2 & \operatorname{Re}(f_{21} f_{22}^*) & -\operatorname{Im}(f_{21} f_{22}^*) \\ 2 \operatorname{Re}(f_{11} f_{21}) & 2 \operatorname{Re}(f_{12} f_{22}^*) & \operatorname{Re}(f_{11} f_{22}^* + f_{12} f_{21}^*) & -\operatorname{Im}(f_{11} f_{22}^* - f_{12} f_{21}^*) \\ 2 \operatorname{Im}(f_{11} f_{21}) & 2 \operatorname{Im}(f_{12} f_{22}^*) & \operatorname{Im}(f_{11} f_{22}^* + f_{12} f_{21}^*) & \operatorname{Re}(f_{11} f_{22}^* - f_{12} f_{21}^*) \end{pmatrix} \tag{72}$$

where the f_{ij} are defined in terms of the scattering functions given in [24]. For spherical particles, the quantities $f_{12} = f_{21} = 0$ and $\underset{\sim}{\bar{\sigma}}$ contains four constants.

Having laid the foundation for the Mie treatment of scattering phenomenon, let us now consider a plane electromagnetic wave incident on an isotropic, homogeneous sphere of arbitrary size. The object interferes with the free propagation of the wave and secondary waves are generated that are predictable by Maxwell's equations and the boundary conditions; and these secondary waves form a scattered radiation field. The incident wave should be linearly polarized for two reasons. First, if the light

is unpolarized, then it can be resolved into two linearly polarized components each of which act independently of the other. One only needs to consider the interaction of the sphere with a plane (linear) polarized wave and then apply the principle of superposition to obtain the total effect. The LIDAR laser pulse is plane polarized, by definition, and this is the wave-type that is considered for tropospheric probing. A geometric diagram of the problem is shown in figure 7, suggesting a spherical coordinate system as the most convenient for analysis.

The fields of electromagnetic energy in the region of space filled by the particle and the incident wave are resolved into three components:

a. the incident wave - $\underset{\sim}{E}_i$, $\underset{\sim}{H}_i$
b. the particle interior wave - $\underset{\sim}{E}_r$, $\underset{\sim}{H}_r$
c. the scattered wave - $\underset{\sim}{E}_s$, $\underset{\sim}{H}_s$

For these quantities to properly define the fields, they must each satisfy Maxwell's equations (1) - (4), the Wave equations (29), (30), and the boundary conditions (19) - (22). The internal field $\underset{\sim}{E}_r$, $\underset{\sim}{H}_r$ must match the external field $\underset{\sim}{E}_i + \underset{\sim}{E}_s$, $\underset{\sim}{H}_i + \underset{\sim}{H}_s$ in accordance with these relations.

Kerker [12] et al., suggests that the derivation deal with the scalar wave equation, (31). Two new functions may be introduced, the electric Hertz vector, $\underset{\sim}{\Pi}_1$, and the magnetic Hertz vector, $\underset{\sim}{\Pi}_2$, and are defined as follows:

$$\underset{\sim}{B}_1 = \mu \varepsilon \nabla \times \frac{\partial}{\partial t} \underset{\sim}{\Pi}_1 \tag{73}$$

$$\underset{\sim}{E}_1 = \nabla\left(\nabla \cdot \underset{\sim}{\Pi}_1\right) - \mu \varepsilon \frac{\partial^2}{\partial t^2} \underset{\sim}{\Pi}_1 \tag{74}$$

$$\underset{\sim}{D}_2 = -\mu \varepsilon \nabla \times \frac{\partial}{\partial t} \underset{\sim}{\Pi}_2 \tag{75}$$

$$\underset{\sim}{H}_2 = \nabla\left(\nabla \cdot \underset{\sim}{\Pi}_2\right) - \mu \varepsilon \frac{\partial^2}{\partial t^2} \underset{\sim}{\Pi}_2 - \sigma \mu \underset{\sim}{\Pi}_2 \tag{76}$$

Scattering of a plane wave by a sphere

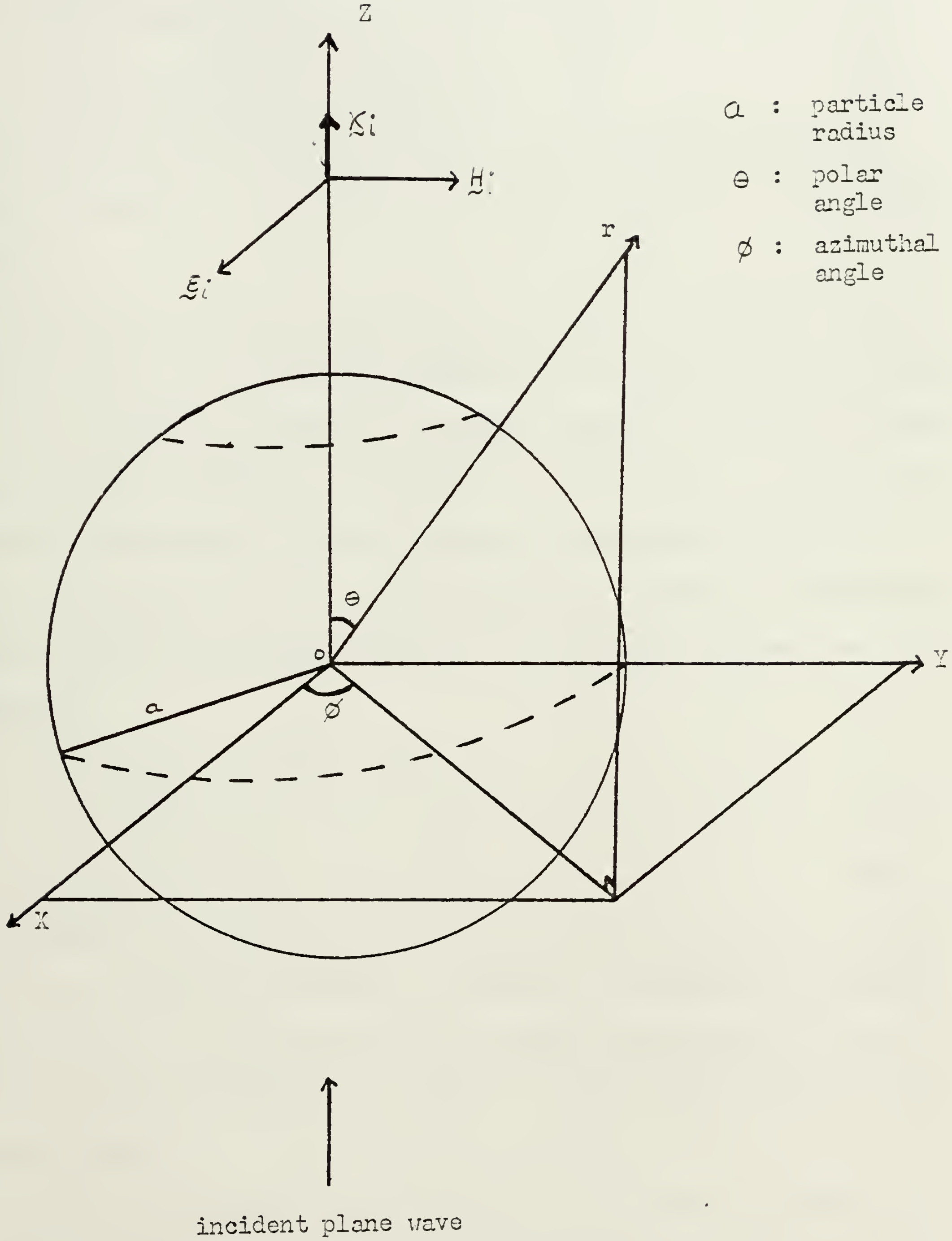

Figure 7

Suitable transformations may be applied to define other Hertz vectors as long as the fields are left invariant. The vectors thus defined must satisfy the vector wave equation:

$$\nabla^2 \underset{\sim}{\Pi}_1 - \sigma\mu \frac{\partial}{\partial t} \underset{\sim}{\Pi}_1 - \varepsilon_0 \mu \frac{\partial^2}{\partial t^2} \underset{\sim}{\Pi}_1 = -\frac{1}{\varepsilon_0} \underset{\sim}{P} \tag{77}$$

$$\nabla^2 \underset{\sim}{\Pi}_2 - \sigma\mu_0 \frac{\partial}{\partial t} \underset{\sim}{\Pi}_2 - \varepsilon \mu_0 \frac{\partial^2}{\partial t^2} \underset{\sim}{\Pi}_2 = -\underset{\sim}{M} \tag{78}$$

where the $\underset{\sim}{P}$ and $\underset{\sim}{M}$ result from distributions of electric and magnetic dipoles. Therefore, two vectors can be used to describe all the fields present.

The transverse magnetic wave (TM), also called the electric wave, has a zero value for the radial component of its magnetic field intensity, $H_{1r} = 0$. Likewise, the transverse electric wave (TE), the magnetic wave, has a zero radial component of electric field intensity, $E_{2r} = 0$. The TM wave is conceived as being the result of oscillating electric dipoles in a spatial region, and the TE wave as the result of oscillating magnetic dipoles. The total solution is a construct of these two wavefronts.

The Hertz-Debye potentials are:

$$-\nabla \cdot \underset{\sim}{\Pi}_1 = \Pi_1 \tag{79}$$

$$-\nabla \cdot \underset{\sim}{\Pi}_2 = \Pi_2 \tag{80}$$

These potentials are the solutions of the scalar wave equation. Solving (79) and (80) for the potentials and applying the appropriate boundary conditions, one can then find the field vectors describing the TM and TE waves. The total field may be derived by the direct addition of the component waves.

The following equations for the total field vector components can be obtained by applying these concepts to the above relations. In spherical

coordinates, we have:

$$E_r = E_{1r} + E_{2r} = \frac{\partial^2}{\partial r^2}(r\Pi_1) + K^2(r\Pi_1) + 0 \qquad (81)$$

$$E_\theta = E_{1\theta} + E_{2\theta} = \frac{1}{r}\frac{\partial^2}{\partial r\partial\theta}(r\Pi_1) + \mathcal{K}_2\frac{1}{r\sin\theta}\frac{\partial}{\partial\phi}(r\Pi_2) \qquad (82)$$

$$E_\phi = E_{1\phi} + E_{2\phi} = \frac{1}{r\sin\theta}\frac{\partial^2}{\partial r\partial\phi}(r\Pi_1) - \mathcal{K}_2\frac{1}{r}\frac{\partial}{\partial\theta}(r\Pi_2) \qquad (83)$$

$$H_r = H_{1r} + H_{2r} = 0 + \frac{\partial^2}{\partial r^2}(r\Pi_2) + K^2(r\Pi_2) \qquad (84)$$

$$H_\theta = H_{1\theta} + H_{2\theta} = -\mathcal{K}_1\frac{1}{r\sin\theta}\frac{\partial}{\partial\phi}(r\Pi_1) + \frac{1}{r}\frac{\partial^2}{\partial r\partial\theta}(r\Pi_2) \qquad (85)$$

$$H_\phi = H_{1\phi} + H_{2\phi} = \mathcal{K}_1\frac{1}{r}\frac{\partial}{\partial\theta}(r\Pi_1) + \frac{1}{r\sin\theta}\frac{\partial^2}{\partial r\partial\phi}(r\Pi_2) \qquad (86)$$

with the propagation constant defined in the following form by (35):

$k^2 = -K_1 K_2$ (87), where $K_1 = i\omega\varepsilon + \sigma$ (88), $\mathcal{K}_2 = i\omega$ (89)

μ has been dropped as all media are assumed to be non-magnetic.

Recalling the scalar wave equation for a function with harmonic time dependence, $e^{i\omega t}$, we have:

(36) $\nabla^2 u + K^2 u = 0$

(34) $u = f(\underset{\sim}{r})e^{i\omega t}$

The spatial part f then satisfies:

$$\nabla^2 f(\underset{\sim}{r}) + K^2 f(\underset{\sim}{r}) = 0 \qquad (90)$$

The Hertz-Debye potentials are constructed such that they are solutions to this wave equation. Let $\Pi(r, \theta, \phi) = f(\underset{\sim}{r})$ represent either potential, Π_1 or Π_2:

$$\nabla^2\Pi + K^2\Pi = 0 \qquad (91)$$

This equation is the one that must be solved; in spherical coordinates:

$$\frac{1}{r}\left(\frac{\partial^2}{\partial r^2} r\Pi\right) + \frac{1}{r^2\sin\theta}\frac{\partial}{\partial\theta}\left(\sin\theta\frac{\partial\Pi}{\partial\theta}\right) + \frac{1}{r^2\sin^2\theta}\frac{\partial^2\Pi}{\partial^2\phi} + K^2\Pi = 0 \qquad (92)$$

It can be solved using the technique of separation of variables, where Π is assumed to be a product function:

$$\Pi(\underset{\sim}{r}) = R(r)\Theta(\theta)\Phi(\phi) \qquad (93)$$

$$\Rightarrow \quad \frac{\partial^2}{\partial r^2}(r\Pi) = \Theta\Phi\frac{d^2}{dr^2}rR \qquad (94)$$

$$\Rightarrow \frac{\partial}{\partial \theta}\left(\sin\theta \frac{\partial \Pi}{\partial \theta}\right) = R\,\Phi \frac{\partial}{\partial \theta}\left(\sin\theta \frac{\partial \textcircled{H}}{\partial \theta}\right) \qquad (95)$$

$$\Rightarrow \frac{\partial^2}{\partial \phi^2}\Pi = R\,\textcircled{H} \frac{\partial^2 \Phi}{\partial \phi^2} \qquad (96)$$

(92) becomes: $\frac{\textcircled{H}\Phi}{r} \frac{\partial^2 rR}{\partial r^2} + \frac{R\Phi}{r^2 \sin\theta} \frac{\partial}{\partial \theta}\left(\sin\theta \frac{\partial \textcircled{H}}{\partial \theta}\right) + \frac{R\textcircled{H}}{r^2 \sin^2\theta} \frac{\partial^2 \Phi}{\partial \phi^2} = -K^2 R \textcircled{H} \Phi$

Since $\Pi \neq 0$, then we multiply by r^2/Π:

$$\frac{r}{R} \frac{\partial^2 rR}{\partial r^2} + \frac{1}{\textcircled{H} \sin\theta} \frac{\partial}{\partial \theta}\left(\sin\theta \frac{\partial \textcircled{H}}{\partial \theta}\right) + \frac{1}{\Phi \sin^2\theta} \frac{\partial^2 \Phi}{\partial \phi^2} = -K^2 r^2$$

$$\Rightarrow \frac{r}{R} \frac{\partial^2}{\partial r^2} rR + K^2 r^2 = -\left[\frac{1}{\textcircled{H} \sin\theta} \frac{\partial}{\partial \theta}\left(\sin\theta \frac{\partial \textcircled{H}}{\partial \theta}\right) + \frac{1}{\Phi \sin^2\theta} \frac{\partial^2 \Phi}{\partial \phi^2}\right] \qquad (97)$$

This equation is equal to a constant which may be checked by taking the derivatives of both sides with respect to r, θ, ϕ. This constant has the form of $n(n + 1)$:

$$\frac{r}{R} \frac{\partial^2}{\partial r^2} rR + K^2 r^2 = n(n+1)$$

Thus the radial equation is:

$$\frac{\partial^2}{\partial r^2} rR(r) + \left[K^2 - \frac{n(n+1)}{r^2}\right] rR(r) = 0 \qquad (98)$$

Using (98), equation (97) becomes:

$$\frac{1}{\textcircled{H} \sin\theta} \frac{\partial}{\partial \theta}\left(\sin\theta \frac{\partial \textcircled{H}}{\partial \theta}\right) + \frac{1}{\Phi \sin^2\theta} \frac{\partial^2 \Phi}{\partial \phi^2} = -n(n+1)$$

$$\left[\frac{\sin\theta}{\textcircled{H}} \frac{\partial}{\partial \theta}\left(\sin\theta \frac{\partial \textcircled{H}}{\partial \theta}\right) + n(n+1)\sin^2\theta\right] = -\frac{1}{\Phi} \frac{\partial^2 \Phi}{\partial \phi^2}$$

By the same differentiation argument, each side of this equation is equal to a constant, m^2:

$$\Rightarrow \frac{\sin\theta}{\textcircled{H}} \frac{\partial}{\partial \theta}\left(\sin\theta \frac{\partial \textcircled{H}}{\partial \theta}\right) + n(n+1)\sin^2\theta = m^2$$

Thus, the θ -angle equation is:

$$\frac{1}{\sin\theta} \frac{\partial}{\partial \theta}\left(\sin\theta \frac{\partial \textcircled{H}(\theta)}{\partial \theta}\right) + \left[n(n+1) - \frac{m^2}{\sin^2\theta}\right] \textcircled{H}(\theta) = 0 \qquad (99)$$

Using (98) and (99), (97) takes the form of:

$$-\frac{1}{\Phi} \frac{\partial^2 \Phi}{\partial \phi^2} = m^2$$

Thus, the ϕ-angular equation is:

$$\frac{\partial^2 \Phi(\phi)}{\partial \phi^2} + m^2 \Phi(\phi) = 0 \qquad (100)$$

In the above equations, n may take on any integer value and m may be any one of the following set: -n, ..., 0, ..., n. Equations (99) and

(100) combine to form the Spherical Harmonics which are defined:

$$Y_n^m(\theta,\phi) = A_n^m \Theta_n^m(\theta)\,\Phi_m(\phi) \tag{101}$$

where A_n^m is a normalization constant to ensure orthonormality of the function set of Y.

The solution to (100) is a straightforward combination of sines and cosines as m^2 is always positive:

$$\Phi_m(\phi) = a_m \cos(m\phi) + b_m \sin(m\phi) \tag{102}$$

Equation (99) is the familiar Associative Legendre equation having the regular solution:

$$\Theta(\theta) = P_n^{(m)}(\cos\theta) \tag{103}$$

where the $P_n^{(m)}(\cos\theta)$ are the associative legendre polynomials. Using Rodrigues' formula [1]:

$$P_n^{(m)}(\cos\theta) = (2^n n!)^{-1}(1-x^2)^{m/2}\,\frac{d^{m+n}}{dx^{m+n}}(x^2-1)^n \tag{104}$$

where $x = \cos\theta$ and the negative values of m are included, $-n \leq m \leq n$. When $m = 0$, then (99) is the legendre equation whose solutions are the legendre polynomials:

$$P_n(x) = (2^n n!)^{-1}\left(\frac{d}{dx}\right)^n (x^2-1)^n \tag{105}$$

Equation (104) may be rewritten as:

$$P_n^{(m)}(x) = (1-x^2)^{m/2}\,\frac{d^m}{dx^m}P_n(x) \tag{106}$$

The complete spherical harmonic solution includes the normalization constant and rewrites the azimuthal solution as a complex exponential. These functions are completely orthonormal as well. Thus:

$$Y_n^m(\theta,\phi) = (-1)^m\sqrt{\frac{2n+1}{4\pi}\,\frac{(n-m)!}{(n+m)!}}\;P_n^{(m)}(\cos\theta)\,e^{im\phi} \tag{107}$$

The $(-1)^m$ term is a phase factor defined as the Condon-Shortly phase, and may, in some texts, be dropped.

(Note: in the remainder of this paper, I will use ζ instead of zeta,

which is used in the literature.)

The Radial equation, (98), has solutions defined in terms of the Bessel functions:

$$\psi_n(kr) = \sqrt{\frac{\pi}{2} kr}\; J_{n+1/2}(kr) \tag{108}$$

$$\chi_n(kr) = -\sqrt{\frac{\pi}{2} kr}\; N_{n+1/2}(kr) \tag{109}$$

$$\Rightarrow \; rR_n(r) = c_n \psi_n(kr) + d_n \chi_r(kr) \tag{110}$$

These are the Ricatti-Bessel functions, where $J_{n+\frac{1}{2}}$ and $N_{n+\frac{1}{2}}$ are the half integral order Bessel and Neumann functions. By using the infinite series definitions of the Bessel functions, one can write the Ricatti-Bessel function in the following derivative form:

$$\psi_n(z) = z^{n+1} \left(\frac{d}{z\,dz}\right)^n \left(\frac{\sin z}{z}\right) \tag{111}$$

$$\chi_n(z) = (-1)^n z^{n+1} \left(\frac{d}{z\,dz}\right)^n \left(\frac{\cos z}{z}\right) \tag{112}$$

where $$z = x + iy \tag{113}$$

The function:

$$\zeta_n(kr) = \psi_n(kr) + i\,\chi_n(kr) = \sqrt{\frac{\pi}{2} kr}\; H^{(2)}_{n+1/2}(kr) \tag{114}$$

vanishes in the limit as kr approaches infinity, and will be useful in later work. The function $H^{(2)}_{n+\frac{1}{2}}(kr)$ is the half integral order Hankel function of the second kind.

Now it can be seen that the solution to the scalar wave equation is characterized by the numbers n, m:

$$r\pi_n^{(m)} = rR_n(r)\,\Theta_n^{(m)}(\theta)\,\Phi_m(\phi)$$

and (102), (103), and (110):

$$\Rightarrow r\pi_n^{(m)}(r,\theta,\phi) = \{c_n\psi_n(kr) + d_n\chi_n(kr)\}\{P_n^{(m)}(\cos\theta)\}\{a_m \cos(m\phi) + b_m \sin(m\phi)\} \tag{115}$$

The general solution may now be obtained as a linear superposition of these particular solutions.

$$r\pi(\underset{\sim}{r}) = \sum_{n=0}^{\infty} \sum_{m=-n}^{n} r\pi_n^{(m)}(r,\theta,\phi) \tag{116}$$

Equation (116) is the general solution of the scalar wave equation in spherical coordinates.

The fields in and about the particle can be described in terms of their individual pairs of potential functions:

a. the incident wave - π_1^i, π_2^i

b. the interior wave - π_1^r, π_2^r

c. the scattered wave - π_1^s, π_2^s

The sphere, whose origin coincides with that of the spherical coordinate system and is of radius a, is isotropic and homogeneous, optically described by a complex propagation constant, k_1:

$$(47) \implies K_1 = m_1 K_0 \qquad (117)$$

The isotropic, homogeneous medium is a dielectric described by a real constant, k_2.

$$K_2 = m_2 K_0 \qquad (118)$$

The relative refractive index is defined:

$$m = K_1/K_2 = m_1/m_2 \qquad (119)$$

The incident plane wave propagates along the positive z-axis and is considered to be of unit amplitude with polarization axis parallel to the x-axis.

$$|\underset{\sim}{E}i| = \left|e^{-iK_2 z}\right| = 1 \qquad (120)$$

In order to facilitate matching the boundary conditions for the Debye potentials on the surface r = a, (120) is written in the form of (116), realizing that the function $\chi_n(k_2 r)$ becomes infinite at the origin where the field (120) does not:

$$r\pi_1^i = \frac{1}{K_2^2} \sum_{n=1}^{\infty} i^{n-1} \frac{2n+1}{n(n+1)} \psi_n(K_2 r) P_n^{(1)}(\cos\theta) \cos\phi \qquad (121)$$

$$r\pi_2^i = \frac{1}{K_2^2} \sum_{n=1}^{\infty} i^{n-1} \frac{2n+1}{n(n+1)} \psi_n(K_2 r) P_n^{(1)}(\cos\theta) \sin\phi \qquad (122)$$

The unperturbed incident wave is now well defined. Because the incident wave propagates along a coordinate axis (z), parameter m = 1. As a result, the Debye potentials all have the associated legendre polynomials of degree 1. The internal particle fields must be of the same form, without $\chi_n(k,r)$, and must also be finite at the origin. Also, the arbitrary coefficients must exist in order to properly map the conditions at the boundary:

$$r\Pi_1^r = \frac{1}{K_1^2}\sum_{n=1}^{\infty} i^{n-1}\frac{2n+1}{n(n+1)}\, c_n \Psi_n(K_1 r)\, P_n^{(1)}(\cos\theta)\cos\phi \tag{123}$$

$$r\Pi_2^r = \frac{1}{K_1^2}\sum_{n=1}^{\infty} i^{n-1}\frac{2n+1}{n(n+1)}\, d_n \Psi_n(K_1 r)\, P_n^{(1)}(\cos\theta)\sin\phi \tag{124}$$

The scattered wave must vanish at infinity without entailing an infinite energy and the function $\zeta_n(kr)$ contributes just this property while maintaining the proper form for $\Pi(\underset{\sim}{r})$. Arbitrary coefficients are again necessary:

$$r\Pi_1^s = -\frac{1}{K_2^2}\sum_{n=1}^{\infty} i^{n-1}\frac{2n+1}{n(n+1)}\, a_n \zeta_n(K_2 r)\, P_n^{(1)}(\cos\theta)\cos\phi \tag{125}$$

$$r\Pi_2^s = -\frac{1}{K_2^2}\sum_{n=1}^{\infty} i^{n-1}\frac{2n+1}{n(n+1)}\, b_n \zeta_n(K_2 r)\, P_n^{(1)}(\cos\theta)\sin\phi \tag{126}$$

The boundary conditions at the interface ensure the continuity of the tangential components of $\underset{\sim}{E}$ and $\underset{\sim}{H}$. In spherical coordinates, this translates into:

$$E_\theta^{(1)}(r=a) = E_\theta^{(2)}(r=a) \tag{127}$$

$$E_\phi^{(1)}(r=a) = E_\phi^{(2)}(r=a) \tag{128}$$

$$H_\theta^{(1)}(r=a) = H_\theta^{(2)}(r=a) \tag{129}$$

$$H_\phi^{(1)}(r=a) = H_\phi^{(2)}(r=a) \tag{130}$$

where (1) refers to the sphere interior and (2) the exterior. The mixture of terms in Π_1 and Π_2 at first glance makes it difficult to apply the boundary conditions. However, by forming the appropriate linear combinations of (81) - (86), the boundary conditions can be recast into

an equivalent form for the Debye potentials. Define:

$$A = \frac{\partial}{\partial \theta}\left(\sin\theta\, E_\theta\right) + \frac{\partial}{\partial \phi} E_\phi \qquad (131)$$

$$B = \frac{\partial}{\partial \theta}\left(\sin\theta\, H_\theta\right) + \frac{\partial}{\partial \phi} H_\phi \qquad (132)$$

$$C = -\frac{\partial}{\partial \phi} H_\theta + \frac{\partial}{\partial \theta}\left(\sin\theta\, H_\phi\right) \qquad (133)$$

$$D = \frac{\partial}{\partial \phi} E_\theta - \frac{\partial}{\partial \theta}\left(\sin\theta\, E_\phi\right) \qquad (134)$$

Then the boundary conditions (127) - (130) become:

$$A^{(1)}(r=a) = A^{(2)}(r=a) \qquad (135)$$

$$B^{(1)}(r=a) = B^{(2)}(r=a) \qquad (136)$$

$$C^{(1)}(r=a) = C^{(2)}(r=a) \qquad (137)$$

$$D^{(1)}(r=a) = D^{(2)}(r=a) \qquad (138)$$

Note that: $$\Pi^{(1)} = \Pi^{r} \qquad (139)$$

$$\Pi^{(2)} = \Pi^{i} + \Pi^{s} \qquad (140)$$

The quantities A and C remove $r\Pi_2$ and B and D remove $r\Pi_1$. The decoupled equations then result in boundary conditions on the Debye potentials.

Substituting (81) - (86) into (131) - (134) yields:

$$rA = \cos\theta \frac{\partial}{\partial \theta}\left[\frac{\partial}{\partial r}(r\Pi_1)\right] + \sin\theta \frac{\partial^2}{\partial \theta^2}\left[\frac{\partial}{\partial r}(r\Pi_1)\right] + \frac{1}{\sin\theta}\frac{\partial^2}{\partial \phi^2}\left[\frac{\partial}{\partial r}(r\Pi_1)\right] \qquad (141)$$

$$rB = \cos\theta \frac{\partial}{\partial \theta}\left[\frac{\partial}{\partial r}(r\Pi_2)\right] + \sin\theta \frac{\partial^2}{\partial \theta^2}\left[\frac{\partial}{\partial r}(r\Pi_2)\right] + \frac{1}{\sin\theta}\frac{\partial^2}{\partial \phi^2}\left[\frac{\partial}{\partial r}(r\Pi_2)\right] \qquad (142)$$

$$rC = \cos\theta \frac{\partial}{\partial \theta}\left[\mathcal{K}_1 r\Pi_1\right] + \sin\theta \frac{\partial^2}{\partial \theta^2}\left[\mathcal{K}_1 r\Pi_1\right] + \frac{1}{\sin\theta}\frac{\partial^2}{\partial \phi^2}\left[\mathcal{K}_1 r\Pi_1\right] \qquad (143)$$

$$rD = \cos\theta \frac{\partial}{\partial \theta}\left[\mathcal{K}_2 r\Pi_2\right] + \sin\theta \frac{\partial^2}{\partial \theta^2}\left[\mathcal{K}_2 r\Pi_2\right] + \frac{1}{\sin\theta}\frac{\partial^2}{\partial \phi^2}\left[\mathcal{K}_2 r\Pi_2\right] \qquad (144)$$

For equation (135) - (138) to be valid for all θ, ϕ on the coordinate surface, $r = a$, requires the various bracketed arguments in (141) - (144) to be equivalent between regions (1) and (2). Thus:

$$\left[\frac{\partial}{\partial r}(r\Pi_1)\right]^{(1)}_{r=a} = \left[\frac{\partial}{\partial r}(r\Pi_1)\right]^{(2)}_{r=a} \qquad (145)$$

$$\left[\frac{\partial}{\partial r}(r\Pi_2)\right]^{(1)}_{r=a} = \left[\frac{\partial}{\partial r}(r\Pi_2)\right]^{(2)}_{r=a} \qquad (146)$$

$$\left[\mathcal{K}_1 r\Pi_1\right]^{(1)}_{r=a} = \left[\mathcal{K}_1 r\Pi_1\right]^{(2)}_{r=a} \qquad (147)$$

$$\left[\mathcal{K}_2 r\Pi_2\right]^{(1)}_{r=a} = \left[\mathcal{K}_2 r\Pi_2\right]^{(2)}_{r=a} \qquad (148)$$

Now, using (139) and (140):

$$\frac{\partial}{\partial r}\left[r\Pi_1^r\right] = \frac{\partial}{\partial r}\left[r(\Pi_1^i+\Pi_1^s)\right] \tag{149}$$

$$\frac{\partial}{\partial r}\left[r\Pi_2^r\right] = \frac{\partial}{\partial r}\left[r(\Pi_2^i+\Pi_2^s)\right] \tag{150}$$

$$\mathcal{K}_1^{(1)} r\Pi_1^r = \mathcal{K}_1^{(2)} r(\Pi_1^i+\Pi_1^s) \tag{151}$$

$$\mathcal{K}_2^{(1)} r\Pi_2^r = \mathcal{K}_2^{(2)} r(\Pi_2^i+\Pi_2^s) \tag{152}$$

Equations (149) - (152) are the required boundary conditions on the Debye potentials. Substitute (121), (123), and (125) into (151):

$$\frac{K_1^{(1)}}{K_1^2}\sum_{n=1}^{\infty} i^{n-1}\frac{2n+1}{n(n+1)}c_n\Psi_n(K_1a)P_n^{(1)}(\cos\theta)(\cos\phi) = \frac{K_1^{(2)}}{K_2^2}\sum_{n=1}^{\infty} i^{n-1}\frac{2n+1}{n(n+1)}\left[\Psi_n(K_2a)-a_n\zeta_n(K_2a)\right]P_n^{(1)}(\cos\theta)\cos\phi$$

Since all terms in the series expansion are linearly independent of each other for each value of n and for all θ, ϕ; then the corresponding terms in the series must be equal:

$$\frac{\mathcal{K}_1^{(1)}}{K_1^2}c_n\Psi_n(K_1a) = \frac{\mathcal{K}_1^{(2)}}{K_2^2}\left[\Psi_n(K_2a)-a_n\zeta_n(K_2a)\right]$$

$$c_n\Psi_n(K_1a) = \frac{K_1^2\mathcal{K}_1^{(2)2}}{K_2^2\mathcal{K}_1^{(1)}}\left[\Psi_n(K_2a)-a_n\zeta_n(K_2a)\right]$$

The quantity $\frac{K_1^2\mathcal{K}_1^{(2)}}{K_2^2\mathcal{K}_1^{(1)}}$ can be reduced by using equations (87), (89), and, recalling that the frequency of an electromagnetic wave is unchanged in traversing the interface:

$$\frac{K_1^2}{K_2^2}\frac{\mathcal{K}_1^{(2)}}{\mathcal{K}_1^{(1)}} = \frac{-\mathcal{K}_1^{(1)}\mathcal{K}_2^{(2)}\mathcal{K}_1^{(2)}}{-\mathcal{K}_1^{(2)}\mathcal{K}_2^{(2)}\mathcal{K}_1^{(1)}} = \frac{\mathcal{K}_2^{(2)}}{\mathcal{K}_2^{(2)}} = \frac{iw}{iw} = 1$$

Applying similar arguments to the remaining boundary condition yields a term of the form: $\frac{K_1}{K_2} = \frac{m_1K_0}{m_2K_0} = m_1/m_2 = m$

The four boundary conditions then become:

$$c_n\Psi_n'(K_1a) = m\left[\Psi_n'(K_2a)-a_n\zeta_n'(K_2a)\right] \tag{153}$$

$$d_n\Psi_n'(K_1a) = m\left[\Psi_n'(K_2a)-b_n\zeta_n'(K_2a)\right] \tag{154}$$

$$c_n\Psi_n(K_1a) = \left[\Psi_n(K_2a)-a_n\zeta_n(K_2a)\right] \tag{155}$$

$$d_n\Psi_n(K_1a) = \left[\Psi_n(K_2a)-b_n\zeta_n(K_2a)\right]m^2 \tag{156}$$

Note: $\Psi'(Kr) = \frac{d}{d(Kr)}\Psi(Kr)$

This set of equations uniquely determines the coefficients a_n, b_n, c_n,

and d_n. However, only those corresponding to the scattered wave are important here. Define the following parameters:

$$\alpha = K_2 a = 2\pi \frac{a}{\lambda} = 2\pi \frac{m_2 a}{\lambda_0} \tag{157}$$

$$\beta = K_1 a = m K_2 a = 2\pi \frac{m_1 a}{\lambda_0} = m\alpha \tag{158}$$

where λ_0 is the vacuum wavelength.

The quantity α is called the dimensionless size parameter. Solve for c_n from (155) and use the result in (153). Also solve for d_n from (156) and use the value in (154). We obtain:

$$a_n = \frac{\psi_n(\alpha)\psi_n'(\beta) - m\psi_n(\beta)\psi_n'(\alpha)}{\zeta_n(\alpha)\psi_n'(\beta) - m\psi_n(\beta)\zeta_n'(\alpha)} \tag{159}$$

$$b_n = \frac{m\psi_n(\alpha)\psi_n'(\beta) - \psi_n(\beta)\psi_n'(\alpha)}{m\zeta_n(\alpha)\psi_n'(\beta) - \psi_n(\beta)\zeta_n'(\alpha)} \tag{160}$$

All the field vectors are now uniquely described given the known parameters m and α. This data enables the coefficients a_n, b_n, c_n, and d_n to be computed and their potentials determined. Finally, the vectors are obtained from (81) - (86). The formal solution is complete. Practical light scattering observations are performed in the far field, or wave zone. This condition is such that $k_2 r \gg n$ where n is the Ricatti-Bessel function's order parameter. In this approximation, the previous relations become simpler. The asymptotic expansion of the Hankel function becomes [1]:

$$\zeta_n(K_2 r) = i^{(n+1)} e^{-iK_2 r} \tag{161}$$

$$\zeta_n'(K_2 r) = i^{n} e^{-iK_2 r} \tag{162}$$

The fields become transverse due to the radial component decay as $(\lambda/r)^2$ compared to the (λ/r) dependence for the non-radial components. Finally, using (81) - (86) with (125), (126) and (161), (162) for the scattered wave only (the $\psi_n(k_2 r)$ tends to zero for large $k_2 r$ with respect to $\zeta_n(k_2 r)$ as does ψ_n') yields:

$$E_{\phi} = \frac{H_{\theta}}{m_2} = -i\,\frac{e^{-iK_2 r}}{K_2 r} \,\mathrm{SIN}\,\phi\; S_1(\theta) \tag{163}$$

$$E_{\theta} = \frac{-H_{\phi}}{m_2} = i\,\frac{e^{-iK_2 r}}{K_2 r} \cos\phi\; S_2(\theta) \tag{164}$$

where the amplitude functions are:

$$S_1(\theta) = \sum_{n=1}^{\infty} \frac{2n+1}{n(n+1)} \left\{ a_n \pi_n(\cos\theta) + b_n \tau_n(\cos\theta) \right\} \tag{165}$$

$$S_2(\theta) = \sum_{n=1}^{\infty} \frac{2n+1}{n(n+1)} \left\{ a_n \tau_n(\cos\theta) + b_n \pi_n(\cos\theta) \right\} \tag{166}$$

and the angular functions are:

$$\pi_n(\cos\theta) = \frac{P_n^{(1)}(\cos\theta)}{\mathrm{SIN}\,\theta} \tag{167}$$

$$\tau_n(\cos\theta) = \frac{d}{d\theta} P_n^{(1)}(\cos\theta) \tag{168}$$

The energy flow in the scattered wave can be calculated by using Poynting's theorem:

$$S = 1/2\left(E_{\theta} H_{\phi}^{*} - E_{\phi} H_{\theta}^{*}\right) \tag{169}$$

where * represents the complex conjugate of the quantity. The intensity function is defined as follows:

$$i(\theta) = |S(\theta)|^2 \tag{170}$$

The intensity of the scattered radiation for unit incident intensity polarized in the ϕ and θ direction are:

$$I_{\theta} = \frac{\lambda^2}{4\pi^2 r^2} \cos^2\phi\; i_2 \tag{171}$$

$$I_{\phi} = \frac{\lambda^2}{4\pi^2 r^2} \mathrm{SIN}^2\phi\; i_1 \tag{172}$$

Note that the intensity decays as $1/r^2$ as it should for this spherically spreading wave. The scattering plane is defined as that plane which contains the incident direction and the direction of the scattered wave (θ,ϕ). Then i_1 is the wave perpendicular to the plane and i_2 is the wave parallel to it. The phase relation between E_{θ} and E_{ϕ} being arbitrary is the condition that defines an elliptically polarized wave. Intuitively, one can think of each polarized component coming from that direction as being inherent in the incident wave. Therefore, the I_{θ} is

caused by an incident wave of intensity $\cos^2\phi$ polarized parallel to the scattering plane.

The phase difference that exists between these two parts of the scattering wave is:

$$\tan\delta = \frac{Re(S_1)Im(S_2) - Re(S_2)Im(S_1)}{Re(S_1)Re(S_2) + Im(S_1)Im(S_2)} \tag{173}$$

Unpolarized incident light gives rise to a scattered beam of intensity:

$$I_u = \frac{\lambda^2}{8\pi^2 r^2}\left(i_1 + i_2\right) \tag{174}$$

with degree of polarization given by:

$$P = \left|\frac{i_1 - i_2}{i_1 + i_2}\right| \tag{175}$$

Fixing the scattering plane in space to be the yz-plane, all observations by definition take place in the scattering plane. The incident electric vector has its direction in the xy-plane at an angle χ to the y-azis. The x-axis is designated vertical and the yz-plane horizontal. This is shown in figure 8. Thus, the vertical (V) and horizontal (H) components of the intensity in the scattered wave for unit incidence become:

$$I_\phi = I_V(\chi) = \frac{\lambda^2}{4\pi^2 r^2}\, i_1 \sin^2\chi \tag{176}$$

$$I_\theta = I_H(\chi) = \frac{\lambda^2}{4\pi^2 r^2}\, i_2 \cos^2\chi \tag{177}$$

The Stokes parameters are:

$$S_0 = \frac{\lambda^2}{4\pi^2 r^2}\left(i_1 \sin^2\chi + i_2 \cos^2\chi\right) \tag{178}$$

$$S_1 = \frac{\lambda^2}{4\pi^2 r^2}\left(i_1 \sin^2\chi - i_2 \cos^2\chi\right) \tag{179}$$

$$S_2 = \frac{\lambda^2}{2\pi^2 r^2}\sqrt{i_1 i_2}\;\sin\chi\,\cos\chi\,\cos\delta \tag{180}$$

$$S_3 = \frac{\lambda^2}{2\pi^2 r^2}\sqrt{i_1 i_2}\;\sin\chi\,\cos\chi\,\sin\delta \tag{181}$$

When discussing cross sections, one is speaking of the amount of area that the particle effectively presents to the incident beam by its ability to spread out the incident energy. The complex index of

Scattering plane geometry

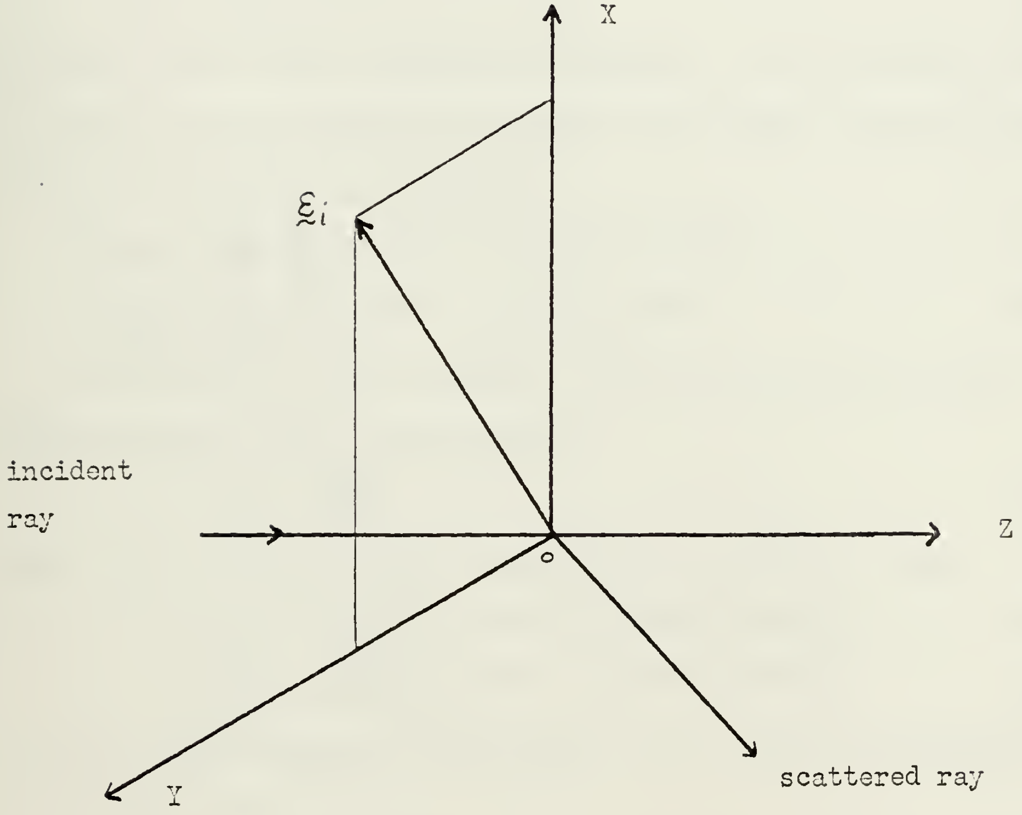

Figure 8

refraction includes absorption as well as scattering. Define the extinction cross section as the sum of the cross sections for scattering and absorption :

$$\sigma_{ext} = \sigma_{sca} + \sigma_{abs} \tag{182}$$

By integrating the real part of the time averaged Poynting vector for the total external field:

$$\underset{\sim}{S} = (\underset{\sim}{E}^i + \underset{\sim}{E}^s) \times (\underset{\sim}{H}^i + \underset{\sim}{H}^s) \tag{183}$$

the total outward flow of energy is obtained. For unit incident energy, the various energy losses represented by the integral resulting from above are the desired cross sections:

$$\sigma_{sca} = \frac{\lambda^2}{2\pi} \sum_{n=1}^{\infty} (2n+1) \left\{ |a_n|^2 + |b_n|^2 \right\} \tag{184}$$

$$\sigma_{ext} = \frac{\lambda^2}{2\pi} \sum_{n=1}^{\infty} (2n+1) \left\{ Re\,(a_n + b_n) \right\} \tag{185}$$

The efficiency factor is defined as the cross section per unit geometrical area (πa^2) of the particle:

$$Q = \frac{\sigma}{\pi a^2} \tag{186}$$

Terms of the form $\frac{\lambda^2}{2\pi} \times \frac{1}{\pi a^2}$ become $\frac{2}{\alpha^2}$ since $\alpha = 2\pi a/\lambda$. Thus:

$$Q_{sca} = \frac{2}{\alpha^2} \sum_{n=1}^{\infty} (2n+1) \left\{ |a_n|^2 + |b_n|^2 \right\} \tag{187}$$

$$Q_{ext} = \frac{2}{\alpha^2} \sum_{n=1}^{\infty} (2n+1) \left\{ Re\,(a_n + b_n) \right\} \tag{188}$$

Note that σ_{sca} and σ_{ext} are independent of the state of polarization of the incident wave.

Kerker [12] et al., gives an excellent review of the difficulties involved in the numerical computation of the previously listed scattering functions. The functions needed to be evaluated are a_n, b_n, π_n, τ_n. Some discussion of the equations is given in the Appendix.

Using approximations for small arguments, the fourth power law attributed to Rayleigh scattering can be directly obtained. The first three scattering coefficients are:

$$a_1 = \tfrac{2}{3}\, i \left(\frac{m^2-1}{m^2+2}\right) \alpha^3 \tag{189}$$

$$a_2 = \frac{1}{15}\, i \left(\frac{m^2-1}{2m^2+3}\right) \alpha^5 \tag{190}$$

$$b_1 = \frac{-1}{45}\, i \,(m^2-1)\, \alpha^5 \tag{191}$$

plus terms in higher powers of α. For the Rayleigh criterion $\alpha << 1$, only a_1 contributes. From the Appendix:

$$\pi_1 (\cos \theta) = 1 \tag{192}$$

$$\tau_1 (\cos \theta) = \cos \theta \tag{193}$$

(165), (166): $S_1(\theta) = \frac{3}{2} a_1 \pi_1 (\cos \theta)$

$S_2(\theta) = \frac{3}{2} a_1 \tau_1 (\cos \theta)$

(170): $i_1 (\theta) = \frac{9}{4} |a_1|^2$

$i_2(\theta) = \frac{9}{4} |a_1|^2 \cos^2 \theta$

For unpolarized incident light, for example, sunlight;

(174): $I_u = \frac{\lambda^2}{8\pi^2 r^2} \frac{9}{4} |a_1|^2 (1 + \cos^2 \theta)$

(189): $I_u = \frac{9\lambda^2}{32\pi^2 r^2} \frac{4}{9} \left|\frac{m^2-1}{m^2+2}\right|^2 \alpha^6 (1 + \cos^2 \theta)$

(157): $I_u = \frac{\lambda^2}{8\pi^2 r^2} \left(2\pi \frac{a}{\lambda}\right)^6 \left|\frac{m^2-1}{m^2+2}\right|^2 (1 + \cos^2 \theta)$

$$\Longrightarrow I_u = \frac{8\pi^4 a^6}{r^2 \lambda^4} \left|\frac{m^2-1}{m^2+2}\right|^2 (1 + \cos^2 \theta) \tag{194}$$

This equation accurately predicts the blue sky phenomenon as the shorter wavelengths scatter much more than the other visible wavelengths in daylight. Equation (175) yields the observed degree of polarization:

$$P = \left| \frac{|a_1|^2 - |a_1|^2 \cos^2 \theta}{|a_1|^2 + |a_1|^2 \cos^2 \theta} \right|$$

$$P = \frac{1 - \cos^2 \theta}{1 + \cos^2 \theta} \tag{195}$$

A plot of this function on a polar graph indicates a maximum of 1, complete polarization, at a scattering angle of 90°. This has long been observed in the day sky. The error associated with the truncation after $n = 1$ is 5% if a/λ is kept $\lesssim 0.05$. This limit is the required Rayleigh criterion.

The cross sections and efficiencies represented by equations (184)-(188) give the total integrated differential cross section with the integral formed over the entire solid angle sphere about the particle. The differential cross section is:

$$\frac{d\sigma}{d\Omega}(\Omega) = \eta_s / \eta_i \tag{196}$$

where: η_s - number of photons scattered into a solid angle per unit time per particle

η_i - number of photons crossing a unit area per unit time

$d\Omega = \sin\theta \, d\theta \, d\phi$, the differential solid angle

The intensity is obtained by multiplying the number of photons at frequency ν by Planck's constant, h, as $h\nu$ is the energy per photon.

$$h = 6.6262 \times 10^{-34} \text{ Joule/sec} \tag{197}$$

As written, equation (196) describes a scattered energy per incident intensity. The scattered energy becomes a scattered intensity when divided by the distance to the observation point, squared, for then the solid angle becomes the subtended area.

$$dA = r^2 \, d\Omega \tag{198}$$

Utilizing the above,

$$dI = \frac{d\sigma}{dA} \tag{199}$$

where dI represents the scattered intensity over dA per unit incident intensity. The equations describing such an intensity, (171) and (172), may be cast in the form:

$$I = \frac{\lambda^2}{4\pi^2 r^2} g(\phi) i(m, \alpha, \theta) \tag{200}$$

where $g(\phi) = \cos^2\phi$ or $\sin^2\phi$

$i(m, \alpha, \theta) = i_1$ or i_2

I is the dI per unit intensity

Thus:

$$\Rightarrow d\sigma = (\lambda^2/4\pi^2)\, i(m,\alpha,\theta)\, g(\phi)\, d\Omega \qquad (201)$$

This equation, when integrated over all angles θ, ϕ yields the cross section given in equations (184) and (185). Hereafter, the symbol σ will mean $d\sigma/d\Omega$ as defined by (201). This is in keeping with the notation in the literature.

$$\sigma(m,\alpha,\theta,\phi) = \frac{\lambda^2}{4\pi^2}\, i(m,\alpha,\theta)\, g(\phi) \qquad (202)$$

This area represents the scattered energy per particle per unit intensity.

The theory may now be extended to multiple particle systems with the addition of the following definitions. Let n be the total number of particles in a region of differentiable volume, cross-sectional area and extent given by dV, dA, and dx respectively.

Then:

$$dV = dxdA \qquad (203)$$

and

$$n = NdV = NdxdA \qquad (204)$$

where N - particle number density

Assume the scattering to be incoherent among the particles. Then the total σ for all the particles is just

$$\sigma_T = n\sigma \qquad (205)$$

where σ - scattered energy per unit intensity for one particle

The amount of intensity scattered into dA is the scattered energy divided by dA.

$$\frac{\sigma n}{\partial A} = \frac{\text{scattered intensity}}{\text{unit incident intensity}} \qquad (206)$$

Another useful parameter is the scattering coefficient:

$$\beta = \frac{\text{scattering intensity}}{\text{incident intensity-path length}} \qquad (207)$$

where the path length dx is that traversed by the incident radiation. Combining the above equations:

$$\beta\, dx = \frac{\sigma n}{dA} = \frac{\sigma}{dA} N\, dx\, dA$$

$$\Rightarrow \quad \beta = \sigma N \tag{208}$$

Until now, r represented the radius of the radiation field and a the particle radius. Again, to be consistent with the literature, r must be assigned to the particle radius. Using the new notation, if there exists a population of scattering centers each described by N(r), then the amount of scattering from all the particles of radius r between r and r + dr is:

$$d\beta = \sigma(m, \lambda, r, \theta, \phi)\, dN(r) \tag{209}$$

The quantity dN(r) may be written as:

$$dN(r) = \frac{dN}{dr}\, dr \tag{210}$$

where $\frac{dN}{dr}$ is the particle number density per particle radius. Then:

$$d\beta = \sigma \left(\frac{dN}{dr}\right) dr \tag{211}$$

Let the lower and upper radii limits be r_1 and r_2 respectively; we have:

$$\beta = \int_{r_1}^{r_2} \sigma(m, \lambda, r, \theta, \phi) \left(\frac{dN(r)}{dr}\right) dr \tag{212}$$

In the case of $\sigma = \sigma_{ext}$, then $\beta = \beta_{ext}$, the extinction coefficient for a volume of scattering particles defined by dV and equation (212) would represent the total energy loss by an incident beam passing through a volume of depth dx. Assuming an x (path length) dependence for $\frac{dN(r)}{dr}$, then the amount of intensity lost per unit incident intensity is:

$$\frac{dI(x)}{I(x)} = -\beta(x)\, dx \tag{213}$$

$$I(x) = I_0 \exp\left\{-\int_0^x \beta(s)\, ds\right\} \tag{214}$$

where I_0 is the incident intensity to the volume at $x=0$. This last equation is known as Bouguer's law. [23] It describes the degradation of the incident beam as it traverses a material path. In order to express the scattered intensity into a solid angle $d\Omega$, we recall that the intensity scattered per particle into solid angle $d\Omega$ was given by equation (200). Let the parameter r in that equation be replaced by R as r now describes the particle radius.

$$I = \frac{\lambda^2}{4\pi^2 R^2}\, i(m,\alpha,\theta)\, g(\phi) \tag{215}$$

As before, the number of particles in the cell, N, applied to equation (215) yields the total scattered intensity per unit radii per volume; then, for all particles of radius r between r_1 and r_2:

$$I = \frac{\lambda^2}{4\pi^2 R^2} \int_{r_1}^{r_2} i(m,\alpha,\theta)\, g(\phi) \left(\frac{dN}{dr}\right) dr \tag{216}$$

$$\Longrightarrow\ I = I(m,\theta,\phi)$$

For unpolarized radiation:

$$i(m,\alpha,\theta)\, g(\phi) = \frac{1}{2}\left(i_1 + i_2\right) \tag{217}$$

where i_1 and i_2 are given by equations (165) - (168) and (170). For the polarized radiation:

$$i(m,\alpha,\theta)\, g(\phi) = \tfrac{1}{2}\left(i_1 \sin^2\phi + i_2 \cos^2\phi\right) \tag{218}$$

Equations (212) and (216) are the specific results of the theory used to investigate aerosol parameters and will be discussed in the next two sections of this paper. First, some comments on the collective scattering phenomenon are in order. It is well known that the more ordered the scattering centers become, the more coherent the scattering due to the phase relations between sites. [18] This leads to a reduced backscatter with corresponding increase in forward scattering. In crystalline substances, there is essentially no backscatter, when off-

resonance; and the incident beam merely undergoes propagation velocity changes. The condition met by a gas at atmospheric pressure or less, where the number density is low on a radiation wavelength scale, ensures that the scattering is incoherent, allowing the summing of intensities from all the scattering centers. The Mie theory for a collection of particles requires a random distribution of scattering sites to achieve this incoherent intensity accumulation. Quantitatively, the near-field interactions between the particle may be ingored if the average distance between sites is at least ten times their radius. This criterion is satisfied even for very dense fogs and the independent scattering model computations are valid for practical tropospheric scattering. However, significant number densities will lead to a large flux of previously scattered light in the region and add multiple scattering effects to the received signal. A quick check on the validity of the single scatterer model is to verify linearity between the observed effects, I and β, and the number density of scattering particles. If the relation is non-linear, one must suspect the existance of coherent and/or multiple scattering. Alternatively, if the relationship is linear, it is certain that the independent, single scattering conditions are present. A measure of this condition may be obtained from equation (214). [24] Let:

$$\tau_x = -\int_0^x \beta(s)\,ds \qquad (219)$$

be the optical depth of the medium, then:

$$I(x) = I_0 e^{-\tau x} \qquad (220)$$

The conditions are:

$\tau_x < 0.1$ (transmission >90%) - single scattering predominates

$0.1 \leq \tau_x < 0.3$ (transmission 75 to 95%) - multiple scattering effects may be removed via correction to the

single scatter model

$0.3 \leq \tau_x$ (transmission $< 75\%$) - the complete, non-analytic, approximate multiple scattering theory applies

Virtually all aerosols in the troposphere satisfy the first criterion.

The literature abounds with material containing graphs of the Mie scattering functions for many specific cases. The Appendix outlines one such case for a specified set of conditions. However, some general information can be reduced from this plethora of data. The amount of forward scattering is about equal to that of the backscattering at a size parameter (α) equal to 0.01. As α is increased, the amount of forward scattering also increases with a like decrease in the backscatter. At $\alpha = 1$, the forward scatter is on the order of 100 times that of the backscatter. Increasing α still further, there exists a unique scattering maximum with the existence of smaller subsequent maxima and minima. The scattering function increases smoothly as α^4 (Rayleigh) up until $\alpha \sim 0.5$. Thereafter, the structure is highly dependent on the complex index of refraction. The large oscillations in the behavior as α is varied become smoothed as the absorption index increases. As the number density, as a function of the particle radius, takes on more of a detailed structure, there is a further smoothing in the scattering functions as small differences tend to be averaged out. Conceptually, one has at hand either an actual particle distribution or a specified model of such.

Given $N(r)$, for each r, we can compute the required $I_r(\alpha,\theta)$ and sum the total intensities using $N(r)$ as a weighting distribution. This

total $I(\alpha,\theta)$ then appears as the smoothed function.

Like the scattering function publications, there are also a large quantity of analytical number distribution models in use. The verification and application of these models has been the primary purpose of much of the aerosol experiments conducted in the past 20 years, and the work is continuing today. As computers become faster, real time inversion analysis will lead to a more accurate determination of the "true" number distributions. Two such models shall be mentioned here. Some natural aerosols may be described with a two-parameter function utilizing a multiplicative scaling coefficient, c, and a shaping parameter, ν, as presented by Junge [11] :

$$f(r) = \frac{dN(r)}{d\ r} = cr^{-(\nu+1)} \tag{221}$$

where $\frac{dN(r)}{d\ r}$ is as previously defined in (210) and ν may vary from about 2.2 to 4.0. As an example, for silicates in the 0.1 μm to 10.0 μm range, one may use:

$$r_1 = 0.04\,\mu m\,, \quad r_2 = 10.0\,\mu m\,, \quad \nu = 3$$

Another such model is in reality a set of models that includes the Junge model as a special case. Deirmendjian [4] has proposed:

$$f(r) = \frac{dN(r)}{dr} = ar^{\alpha} e^{-br^{\gamma}} \tag{222}$$

(note: the α used here is different from the size parameter.) The versatility of this approach is the presence of four adjustable parameters (a, α, b, γ) allowing for a wide range of experimental data to be fitted. Three specific cases of this model are:

Haze C (continental): $f \sim r^{-4}$

Haze M (maritime) : $f \sim re^{-b\sqrt{r}}$

Cloud : $f \sim r^{6}e^{-1.5r}$

Most of the other proposed model distributions utilize some form of equation (222) as their basis and canned routines for their computer modelling are readily available.

Two other effects that have been omitted in the present theory are Doppler shifts and Brillouin scattering. The presence of random (thermal) acoustic waves in an atmospheric cell will add a degree of order whereby Brillouin scattering of the incident wave can occur off of the resultant density fluctuations. However, this effect is extremely weak for gaseous materials and the degree of coherence added to the structure of the gas is generally undetectable. Similarly, this motion of the gas will cause Doppler broadening of the wavelength of the incident radiation adding to the natural line width of the source. Even for the sharpest sources, lasers, the natural linewidths are on the order of several MHz. Whereas, for almost all atmospheric conditions, the expected Doppler shifts are on the order of a few tenths of a MHz. Therefore, the shift is generally lost in the natural linewidth and the relative motion between the detector and the atmospheric cell may be neglected.

III. LIDAR

The sophistication of the laser systems available today, coupled with the fast computer processing that can cheaply be obtained, has singled out the laser radar, LIDAR, system for increased use as a tropospheric experimental device. The LIDAR should have the ability to perform a wavelength scan with selectable bandwidth receivers. It is the atmospheric attenuation of the laser pulse and the introduction of

random phase and amplitude changes that combine to form the scattered pulse, or echo. The subsequent inversion of this data then allows the experimenter to assess the optical characteristics of the atmosphere on a real-time basis. With the system geared to perform azimuthal and elevation scanning as well as range gating, one can then map out the atmospheric optical behaviour within the visible hemisphere. The two most important atmospheric parameters to be considered for a pulsed LIDAR system are the extinction and scattering coefficients. The total extinction coefficient may be written:

$$\beta = \beta_R + \beta_m + \beta_A + \beta_0 \qquad (223)$$

where R - Rayleigh (molecular) scattering
M - Mie (aerosol + other) scattering
A - Molecular and Aerosol absorption
O - Other processes (Raman, fluorescence, etc)

The other processes taken together are typically two or more orders of magnitude weaker than the Rayleigh effect and tend to get lost in the signal noise.

Rayleigh scattering is obtained from the Mie solution assuming $\alpha << 1$; using equations (184) and (189) - (191):

$$\sigma_R(sca) = \frac{\lambda^2}{2\pi} 3 \left(\frac{4}{9}\right) \left|\frac{m^2-1}{m^2+2}\right|^2 \alpha^6 \qquad (224)$$

Rayleigh scattering for air molecules assumes m is real and $m \approx 1$; $\alpha = 2\pi a/\lambda$:

$$\sigma_R(sca) = \frac{8}{3}(m^2-1)^2 V^2 \frac{\pi^3}{\lambda^4} \qquad (225)$$

where $V = (4/3)\pi a^3$, the volume of one molecule. Let $N_s = 1/V$, the molecular number density, then:

$$\sigma_R(sca) = \frac{8\pi^3}{3\lambda^4} \frac{(m^2-1)^2}{N_s^2} u g(\theta, \phi) \qquad (226)$$

where $u = (6+3\delta)/(6-7\delta)$, the depolarization factor, required (227) to account for the anisotropy of air molecules, for which $\delta = 0.035$. [23] The quantity

$$g(\theta,\phi) = 0.06071\,(1+0.932\cos^2\theta) \qquad (228)$$

also accounts for the anisotropy. Let ρ_a be the air molecule number density (vice N), then:

$$\beta_R = \rho_a\,\sigma_R(m,\theta) \qquad (229)$$

where it is assumed all air molecules have approximately the same radius of $10^{-4}\,\mu$m.

The Mie extinction coefficient is dependent on particle radius through equation (212) whose only unknown is $dN(r)/dr$. The unique sharp wavelength feature of the LIDAR allows one to work well away from the characteristic absorption lines of the sample. Conversely, it also allows one to type the scatterer composition. For example:

Laser 1: λ_1 on an absorption (resonance) line of a particular species;

$$\Rightarrow \beta_1 = \beta_{R1} + \beta_{m1} + \beta_{A1} + \beta_A' \qquad (230)$$

where β_A' is the resonant absorption extinction coefficient which is strongly dependent on λ with tabulated σ_A' and

$$\beta_A' = \sigma_A'\,\rho' \qquad (231)$$

The ρ' is the number density of the species.

Laser 2: λ_2 just off the resonance;

$$\beta_2 = \beta_{R2} + \beta_{m2} + \beta_{A2} \qquad (232)$$

Due to the relatively weak λ dependence for β_R, β_m, and β_A

$$\beta_1 - \beta_2 \simeq \beta_A' \qquad (233)$$

For an analysis cell a distance R away:

(214) $$I(R) = I_o e^{-\int_0^R \beta(s) ds}$$

and back at the receiver:

$$I'(0) = I(R) e^{-\int_0^R \beta(s) ds} \qquad (234)$$

Then: $$\frac{I_1'}{I_2'} = \frac{I_{01}}{I_{02}} e^{-2\int_0^R \beta \acute{A}(s) ds} \qquad (235)$$

Thus, the ρ' for the particular species may, in principle, be found from this equation using the inversion techniques outlined in the next section. For the typical magnitudes of the considered cross sections, see Table II.

TABLE II

Process	σ (cm^2/ster)
Mie	10^{-27} to 10^{-8}
Rayleigh	10^{-27}
Raman	10^{-30} to 10^{-29}
Resonance Raman	10^{-23}
Fluorescence	$\lesssim 10^{-16}$

Similar to radar in operation, the LIDAR has a performance equation whereby the system characteristics and the appropriate atmospheric parameters whcih contribute to the signal are related.[23] Consider a pulsed LIDAR operating in monostatic mode (receiver/transmitter co-located) being used to analyze a specific atmospheric cell via its optical properties. The problem geometry is outlined in figure 9. In this figure:

h_t - cell height

R - slant range to cell

Ω_r -receiver solid angle

Ω_t - transmitter solid angle

L - cell length "gated" via receiver on-time

Monostatic laser radar

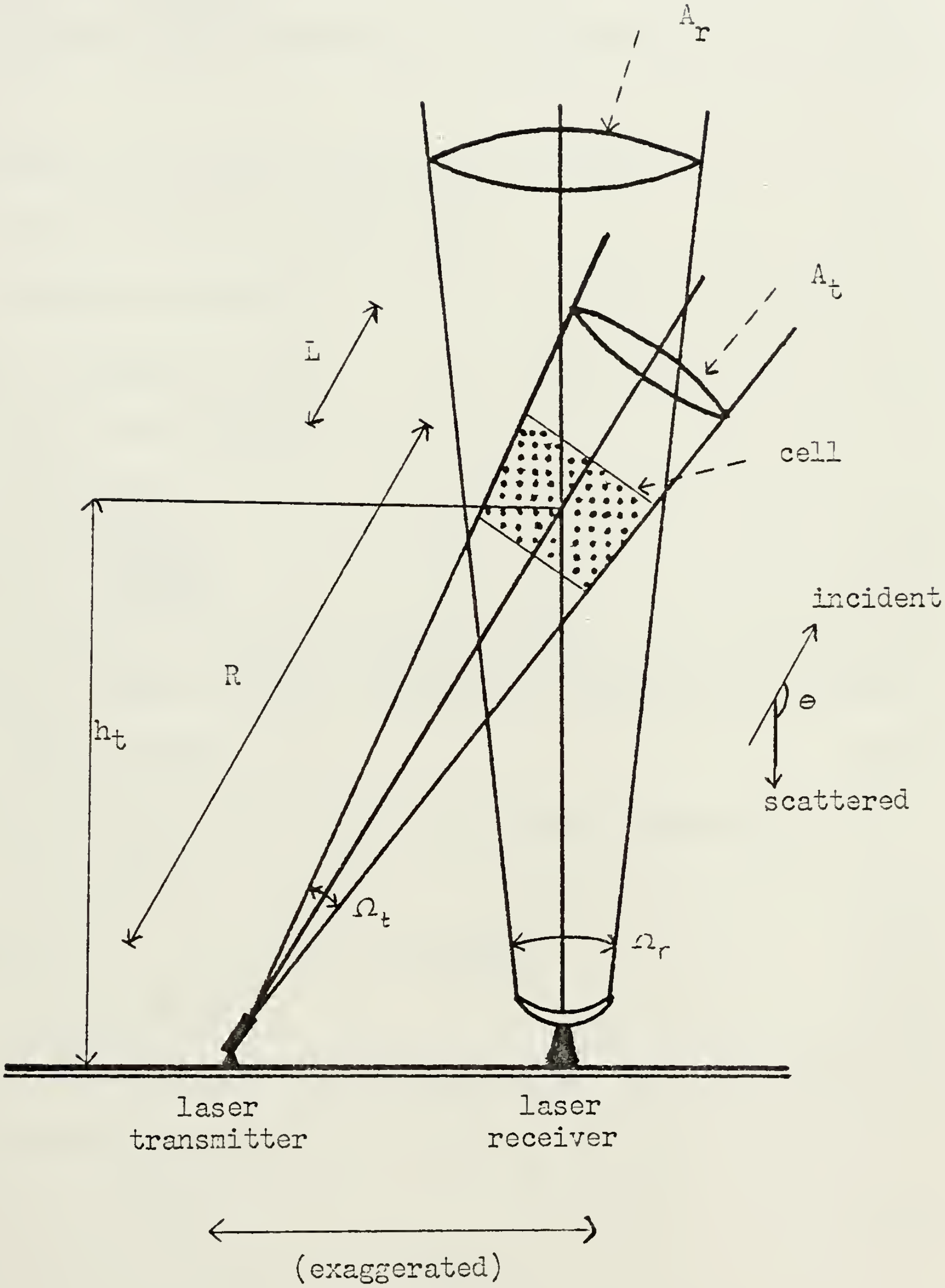

Figure 9

A_r - cell area seen by receiver

A_t - cell area seen by transmitter

The following derivation shall consist of counting photons at each stage along the beam path; converting to intensities has been previously discussed.

1. N_t - number of photons transmitted per pulse

ν_t - photon frequency (transmitted)

$h\nu_t$ - energy per photon

$N_t h\nu_t$ - energy per pulse

P_t - laser output power

τ_t - pulse width

$$\Rightarrow \quad N_t = \frac{P_t \tau_t}{h\nu_t} \tag{236}$$

2. For monostatic LIDAR, the scattering angle is 180 degrees (π) for backscatter. Assume that all backscattered photons are received:

$$\Rightarrow \quad \Omega_R \geqslant \Omega_t \tag{237}$$

The cell volume is determined by the LIDAR timing sequence and is:

$$V = LA_t \tag{238}$$

The solid angle: $\Omega = A/R^2$ (239)

$$V = L\Omega_t R^2 \tag{240}$$

The pulse width constrains the maximum system resolution by limiting the minimum cell length achievable:

$$L_{min} = \tfrac{1}{2}(c\tau_t) \tag{241}$$

where c is the speed of light in the medium.

This condition assumes that the pulse tail reflecting off the front face of the cell does not interfere with the pulse front reflecting off the rear of the cell.

3. N_L - number of photons incident on the cell

β_t - atmospheric extinction coefficient for the given $\lambda_t(\nu_t)$ transmitted

$$N_L = N_t e^{-\int_0^R \beta_t(s)ds} \tag{242}$$

However, to account for beam forming requirements, assume an optical system efficiency of η_t:

$$\Rightarrow \quad N_L = \eta_t N_t e^{-\int_0^R \beta_t(s)ds} \tag{243}$$

4. The backscattering coefficient may be defined in accordance with equation (212):

$$\rho\sigma(\pi) = \beta(\pi) = \int_{r_1}^{r_2} \sigma(m, \lambda_t, r, \theta = \pi, \phi)\left(\frac{dN(r)}{dr}\right)dr \tag{244}$$

where $\rho\sigma(\pi)$ is the usual notation. This equation represents the backscattered intensity per unit incident intensity per unit solid angle per unit path length. The signal returned from the cell is due to this process alone. Bouguers' law (214) states, for $\rho\sigma(\pi)$ assumed constant throughout cell length:

$$I = I_0 e^{-\rho\sigma(\pi)L} \tag{245}$$

where I is that portion of the incident beam that passes through L unaffected. The scattered portion is $I_s = I_0 - I$:

$$N_s = N_L\left(1 - e^{-\rho\sigma(\pi)L}\right) \tag{246}$$

where N_s - the number of photons backscattered and a ratio of intensities is the same as the ratio of the number of photons. Typical tropospheric aerosols yield:

$$\rho\sigma(\pi)L << 1 \tag{247}$$

(if $\rho\sigma(\pi)L = 0.02$, overall error 1%.)

The restriction this places on L is an upper limit of several hundred meters; L_{max}. Thus:

$$1 - e^{-\rho\sigma(\pi)L} \simeq \rho\sigma(\pi)L \tag{248}$$

$$\Rightarrow \quad N_s' = N_L \rho\sigma(\pi)L \tag{249}$$

The prime on N_s indicates the number of photons per solid angle that have been backscattered. Combining equations (243) and (249):

$$N_s' = N_t \eta_t \rho\sigma(\pi)L \exp\left\{-\int_0^R \beta_t(s)\,ds\right\} \tag{250}$$

5. Now the echo must pass through the same propagation path on its return to the receiver as it did on its way to the cell. However, the extinction coefficient may be different, β_r, due to the accumulation of processes like Raman scattering, Brillouin scattering, Doppler shift, etc., though individually negligible.

N_m - number of photons at receiver mirror

$$N_m = N_s' \Omega_r e^{-\int_0^R \beta_r(s)\,ds} \tag{251}$$

(239), (250):

$$N_m = \frac{N_t \eta_t \rho\sigma(\pi) L A_r \exp\left\{-\int_0^R \left[\beta_t(s) + \beta_r(s)\right] ds\right\}}{R^2} \tag{252}$$

6. The optical system will collect the echo photons received at an efficiency of η_r and convert them to an electrical signal via a detector with a quantum efficiency of η_q:

$$N_r = N_m \eta_r \eta_q \tag{253}$$

where N_r - number of photons received and counted per transmitted pulse, due to backscatter from the atmospheric cell of interest.

Thus:

$$N_r = \frac{N_t \eta_t \rho\sigma(\pi) L A_r \eta_r \eta_q \exp\left\{-\int_0^R \left[\beta_t(s) + \beta_r(s)\right] ds\right\}}{R^2} \tag{254}$$

This equation may be recast in the form of intensities if the photon population returned is large enough that individual photons need not be counted. Let D be the optical system aperature (D_t - transmitter; D_r - receiver), then the intensity becomes:

$$I = Nh\nu/D \tag{255}$$

Rewriting equation (254):

$$I_r = \frac{I_t\left(\frac{\nu_r}{\nu_t}\right)\left(\frac{D_t}{D_r}\right)\eta_t\,\rho\,\sigma(\pi)\,L\,A_r\,\eta_r\,\eta_q\,\exp\left\{-\int_0^R\left[\beta_t(s)+\beta_r(s)\right]ds\right\}}{R^2} \tag{256}$$

Thus, the important parameters for the LIDAR analysis of an atmospheric cell are the scatterer number densities and associated cross sections.

For a given system design, one has available the quantities I_t, η_t, η_r, η_q, A_r, D_t, D_r, and can select the values for ν_t, L, and R. If one assumes a slow moving target cell, then the pulse round trip time, t_r, is:

$$t_r = 2R/c \tag{257}$$

$$\Longrightarrow \quad R = (c/2)\,t_r \tag{258}$$

Thus, one determines the range, R, by turning the receiver optics on a time, t_r, after the pulse is emitted. In order to avoid the problem of range ambiguity, like radar, one must ensure that t_r be less than the period between pulses:

$$t_r < 1/PRF \tag{259}$$

where PRF - pulse repetition frequency

The unambiguous range limit may be written;

$$R_u = (c/2)/PRF \tag{260}$$

where R_u - unambiguous range

The cell length, L, is determined by the time that the receiver is turned off again a time Δt after t_r. For the entire cell to be scanned, the pulse must traverse L twice in Δt:

$$L = (c/2)\,\Delta t \tag{261}$$

and the receiver must be turned off at time:

$$t = t_r + \Delta t \tag{262}$$

One can then select L and R by programming a timing sequence for Δt and

t_r. Finally, the interpulse period, T, which is a system deadtime between pulses available for processing, becomes:

$$T = (1/PRF) - \gamma_t \qquad (263)$$

Now one measures I_r and ν_r and applies equation (256) to determine the desired quantities $\rho\sigma(\pi)$ and $\beta(s)$. This inversion is covered in detail in the next section. Note that when the equation for $\sigma(m,\lambda,r,\theta,\phi)$ from (202) is used to replace the $\sigma(m,\lambda,r,\theta,\phi)$ in (244), then equation (256) for I_r has the correct form as given by (216) for the scattered intensities.

Thus, a model has been constructed whereby the system parameters are related to the cell unknowns in a definite manner. But first, some consideration must be given to system noise. During the time the receiver gate is open, Δt, the system will collect and count the background sky photons as well as the signal. The continuous "dark current" in the detector yields an electrical noise as a result of dark counts. These counts arise from photoelectrons being emitted from the detector photocathode surface even without an illumination present. Each of these noise sources may be reduced by proper design of the equipment and experiment. In the case of a detector, its dark current, I_D, is either specified or may be measured in the laboratory:

$$I_D = N_D e G \qquad (264)$$

where N_D - number of dark counts per sec

e - electron charge per count

G - detector count gain

The number of dark counts detected as part of the return signal in a time Δt is $N_D \Delta t$, and :

$$N_D = I_D/(eG) \tag{265}$$

Let N_B represent the background count rate such that $N_B\Delta t$ is the number of background counts received per laser pulse. Assume a background spectral brightness, W_λ, that accounts for all the natural and artificial background sources. This W_λ represents a power density per solid angle in the background sky. Then:

$$N_B = (\eta_q \eta_r) \frac{W_\lambda \Omega_r D_r}{h\nu} \Delta\lambda \tag{266}$$

where $\eta_q, \eta_r, \Omega_r, D_r$ - previously defined

ν - frequency of background photons (at λ)

$\Delta\lambda$ - receiver bandwith, centered about λ

Let N_n be the total number of noise counts per laser pulse; using equation (261) for Δt:

$$N_n = (2L/c)(N_D + N_B) \tag{267}$$

Due to the pulse repitition frequency, PRF, the noise count rate:

$$N = (PRF) N_n \tag{268}$$

where N - noise count rate

The statistical nature of noise yields an effective RMS noise count rate of $\sqrt{N}$. The signal has a count rate of:

$$S_r = (PRF) N_r \tag{269}$$

where S_r - count rate from signal echo alone

Thus, the total counting rate is:

$$S = PRF(N_r + N) \tag{270}$$

Taking the RMS of the signal plus noise, one can form the signal-to-noise ratio:

$$S/N = S_r/\sqrt{S} \tag{271}$$

Assuming a one second time averaging:

$$S/N = \sqrt{PRF}\ N_r / \sqrt{N_r + N_n} \qquad (272)$$

If the noise average, N_n, is not accurately measured, the N_n is replaced by $2N_n$ (measured) in the above equation. Note that:

1. $\text{if } N_n = 0 \Rightarrow (S/N)_0 = \sqrt{(PRF)N_r} \qquad (273)$
2. $\text{if } N_n = N_r \Rightarrow (S/N)_2 = (S/N)_0 / \sqrt{2} \qquad (274)$

Therefore, the S/N ~ PRF and by increasing PRF, one increases the signal-to-noise ratio. However, via equation (260), the unambiguous range decreases faster than the increase in S/N. Since a large S/N is desired with good range resolution, one selects a detector with a low I_D(N_D) and designs the system for low background reception (N_B). If the time averaging had been performed over a period of τ seconds such that PRF τ pulses had been transmitted and received:

$$S/N = \sqrt{PRF\tau}\ N_r / \sqrt{N_r + N_n} \qquad (275)$$

Combining equations (265)-(267) and (275):

$$\frac{S}{N} = \frac{\sqrt{PRF\tau}\ N_r}{\left[N_r + \frac{2L}{c}\left(\frac{I_D}{eG} + \frac{\eta_q \eta_r W_\lambda \Omega_r \Delta\lambda D_r}{h\nu}\right)\right]^{1/2}} \qquad (276)$$

Examination of the above equation and (254) leads one to some general system noise qualifications.

1. One desires a low detector I_D and a high η_q.

2. Select a narrow receiver spectral bandwidth, $\Delta\lambda$; another reason for the choice of a laser.

3. Reducing L reduces the noise as well, but the transmitter must put out greater power to maintain the same signal. Then, for the same average power, the PRF must be lowered and the effect in S/N is only $\sqrt{PRF}$ as compared to the L decrease and N_t increase, increasing S/N. In general, high power/low PRF yields a better S/N than a low power/high PRF.

4. A small Ω_r requires a lower beam divergence at the transmitter and an optical matching between the receiver and the echo beam pattern (another laser capability).

5. Without any noise, there still exists a finite $(S/N)_0$ which represents the "shot noise" statistical nature of the signal. It must be emphasized that all the quantities in equation (276) represent the mean of the indicated variables.

6. If $N_r << N_n \Rightarrow S/N \sim N_r$ (277)

If $N_r \gtrsim N_n \Rightarrow S/N \sim \sqrt{N_r}$ (278)

The actual tropospheric measurement will include both Rayleigh (molecular) and Mie (aerosol) scattering. As an example:

a. single water droplet, $r = 1 \mu m$ (Mie)

$$\sigma_s \sim 10^{-8} \text{ cm}^2$$
$$\rho \sim 10 \text{ cm}^{-3}$$
$$\Rightarrow \beta_m \sim 10^{-7} \text{ cm}^{-1}$$

b. nitrogen and/or oxygen molecule, (Rayleigh)

$$\sigma_s \sim 10^{-28} \text{ cm}^2$$
$$\rho \sim 10^{19} \text{ cm}^{-3}$$
$$\Rightarrow \beta_R \sim 10^{-9} \text{ cm}^{-1}$$

Thus, the addition of β_R to the total β_r is on the order of a few percent and any quantitative measurement must take into account both the aerosol and molecular scattering. The turbidity is defined as the ratio of the total scattering intensity to the Rayleigh scattering intensity:

$$\tau_\lambda = I_T / I_R \qquad (279)$$

Some researchers attempt the measurement of this quantity independent of the intensity, then use the result to deduce the aerosol I_M. Another method assumes that the aerosol concentration above a certain height (e.g. $\gtrsim$ 30 km) is sufficiently low to allow it to be neglected. Then

equation (256):

$$I_R \sim \rho_a \sigma_R(\pi) \qquad (280)$$

Next, one computes I_R^S from (256) assuming the conditions of the U. S. Standard Atmosphere and equation (226). This is the expected echo intensity due to molecular scattering alone. The ratio between the measured I_R and the expected I_R^S yields a scale factor, b, that corrects the standard atmosphere for the local conditions. Using this factor, one assumes a density distribution for the local atmosphere the same as that for the standard and computes the expected value of I_R^S at the cell's location. This intensity is then scaled using b. The measured value of I_T is then corrected for this $I_R^S(b)$ and the result becomes I_M, the Mie intensity:

$$I_M = I_T - bI_R^S \qquad (281)$$

For other means of separating the molecular and aerosol intensities from a measurement, the reader is referred to the work by Hall, et. al. [7] This Rayleigh-atmosphere assumption is the starting point for the inversion process.

The Standard Atmosphere may be represented via the following equations:

temperature $T(°F) = 59.31 - 0.00357\,(°F/ft)\,h(ft)$ (282)

pressure $P(atm) = 1.022\,\exp(-4.157\times 10^{-5}(1/ft)\,h(ft))$ (283)

Mass density (slugs/ft^3) $= 0.002425\,\exp(-3.38\times 10^{-5}(1/ft)\,h(ft))$ (284)

where h may vary from 0 to 37,000 feet. [3] The more precise form for these relations are also represented as canned computer routines.

The critical term in equation (256) is the $\rho_m \sigma_m(\pi)$ where the subscript M refers to the aerosol distribution alone. The extinction component in the exponent of e in this equation represents the scattering

and absorption cross sections integrated over the entire 4π steradian sphere. If one assumes some representative model for the aerosol distribution, as was done for the Rayleigh case, then the only unknown in (256) is $\rho_m \sigma_m(\pi)$. The two averaging processes, integrating aver 4π and integrating along the path R, reduces the sensitivity of the exponential term in (256) on the actual aerosol distribution. After completing the inversion process, one may input the best estimate for this distribution into the exponential term in (256) and then repeat the inversion. However, the processing time involved may prove to be the final constraint.

The LIDAR experiment yields the scattered Mie intensity from the aerosol population in the analyzed atmospheric cell as a function of the pre-selected parpmeters at the laser (e.g. wavelength and polarization scanning). With this data as input, the system is prepared to perform the inversion routine. Some computational needs are reduced for the case of laser backscatter as the scattering angle remains fixed at 180 degrees. This backscattering condition simplifies several calculations as outlined in the Appendix.

IV. MATHEMATICAL INVERSION

The assumption made throughout this paper implies that the experimenter need only apply the exact Mie theory to his observations and perform a simple data inversion to discern the aerosol properties of interest. However, this inversion is by no means simple. Aerosol properties may be separated into two distinct catagories. The first considers those parameters that are explicit in the previously defined scattering functions; i.e., spherical aerosols, aerosol sizes, low

number densities, and the relative indices of refraction. Then there are those aerosol characteristics that require some approximations (in many cases, severe ones) to the theory; i.e., non-spherical shapes, anisotropy of the shapes with respect to the scattering plane, and high number densities leading to multiple scattering effects. The first few LIDAR experiments investigated the actual aerosol ranges for these parameters. They found that in excess of 90% of the real aerosols studied, the spherically symmetric single scattering theory was valid under favorable atmospheric conditions. These conditions require the absence of dense water clouds in the atmospheric cell and a depolarization of the incident beam limited to a maximum of 2%, with 1.5% of less actually measured.[23] In the following analysis, these favorable conditions will be assumed, as will the requirements of single particle scattering. These conditions are enhanced by the common field of view shared by the LIDAR transmitter and receiver.

Recall equation (216) for the scattered intensity a distance R away from a cell containing an aerosol population described by dN/dr with radii limits r_1 to r_2:

$$I = \frac{\lambda^2}{4\pi^2 R^2} \int_{r_1}^{r_2} i(m,\alpha,\theta)\, g(\phi) \left(\frac{dN(r)}{dr}\right) dr \tag{216}$$

The first simplification is to replace the particle radii continuum with a set of distinct particle classes each with a characteristic radius, number density and complex index of refraction. Thus:

$$I = I(m_1, m_2, \cdots, r_1, r_2, \cdots, N_1, N_2, \ldots, \lambda, \theta, \phi) \tag{285}$$

where m_j - j^{th} particle refractive index

r_j - j^{th} particle radius

N_j - j^{th} particle number density

λ - incident radiation wavelength

θ, ϕ - scattering angles

The large number of unknowns that need to be determined will ensure a non-unique inverted solution from the limited sample of observations available. There is also the added difficulty of variance in the supposedly known data whose uncertainties at best generate unbounded noise in the final results. Therefore, some attempt must be made at reducing the initially large number of unknowns.

The dependence of the intensity on the size parameter, has been discussed previously. Briefly, the non-monotonic fluctuations as α is varied is the distinctive feature of the Mie theory that enables the process to be of good use in tropospheric analysis. These maxima and minima are reduced by increasing the field of view and/or the transmitter bandwidth. It is to LIDAR's advantage, then, to retain this complex structure as a data filter. See the Appendix for a sample plot of $Q(\alpha)$.

The complex index of refraction, m, has a dispersion relation like any electromagnetic medium. See Table III for an example.

The less than 1% change in the index of refraction is typical for dielectric media. The change in the absorption, γ, is even less. Studies have indicated that the dispersion in m is balanced by the randomness of the aerosol size distribution in such a manner as to almost negate this dispersion. [23]

The angular dependence is a pre-specified set of conditions, especially for the case of a LIDAR backscatter system. This system consists of a linearly polarized wave undergoing only backscatter observations.

As a result of these and similar considerations, one can reduce the

number of unknowns drastically by making only a few simplifying assumptions. These have also been verified by the laboratory analyses of many aerosol samples, natural and artificial.

TABLE III

Liquid water (@20°C) index dispersion; $m = n(1-i\chi)$

(A°)	n
4046.6	1.342724
4471.5	1.339423
5015.7	1.336363
5460.7	1.334466
5892.6	1.332983
6562.8	1.331151
7065.2	1.330019

1. The measured values for n range from 1.33 to 1.59 with respect to the surrounding air. A large class of aerosols (particulates) may be characterized by:

$$m = 1.54(1 - i0.001) \tag{206}$$

Thus, assume that the complex index of refraction is both known and unique. Only the particle's radius and number density is allowed to vary.

2. Typical non-precipitating aerosols in the troposphere are described with their radii between 0.01μm and 15μm. Their number densities can be represented by distributions containing only a few parameters. The important model distributions were presented earlier and the usual goal of an inversion is to best fit one of them. The initial estimates, where required, of particulate properties usually includes such models.

The set of unknowns reduces to the particle number densities and

their radii. By the use of pre-selected values for r, one only has to solve for the distribution functions granting that the radii range is properly considered. Therefore the parameter of primary interest is the scatterer number density.

Define the Mie function, K:

$$K(m,r,\lambda,\theta,\phi) = \left(\frac{\lambda}{2\pi R}\right)^2 i(m,\alpha,\theta)\, g(\phi) \tag{287}$$

and the particle size distribution function, f(r):

$$f(r) = \frac{dN(r)}{dr} \tag{288}$$

The scattering intensity, equation (216), becomes:

$$I(x) = \int_{r_1}^{r_2} K(x,r)\, f(r)\, dr \tag{289}$$

where x represents the set of user defined parameters $(m, \lambda, \theta, \phi)$. The value I(x) is measured, the quantity K(x,r) is computed and the unknown f(r) must be solved for. This relation is classified as a Fredholm integral equation of the first kind. The kernel of the equation is K(x,r) and I(x) represents the transform of f(r) utilizing the stated kernel. There exists only a finite set of measurements, I(x), over which the inversion may be performed. Let the subscript i represent the i^{th} measurement of a set of n observations:

$$I(x_i) = g(x_i) = g_i = \int_{r_1}^{r_2} K(x_i,r)\, f(r)\, dr \tag{290}$$

The notation, g_i, has been introduced and will be used later in the paper. The inversion process is by nature an unstable one and this may easily be demonstrated.[22] Define:

$$S_F(x_i,f) = \int_0^{\pi} K(x_i,r)\left[f(r) + C \sin Fr\right] dr \tag{291}$$

where $i = 1, 2, \ldots, n$ $F = 1, 2, 3, \ldots$

and C is an arbitrary constant. Letting $r_1 = 0$ and $r_2 = \pi$ in equation (290):

$$S_F(x_i,f) = g(x_i) + C\int_0^{\pi} \sin(Fr)\,K(x_i,r)\,dr \qquad (292)$$

Since the sin(Fr) acts as a weighting function for the kernel on the interval $(0,\pi)$, as F increases without bound, the second integral tends to 0. Thus:

$$S_F(x_i,f) \xrightarrow[F\to\infty]{} g(x_i) \qquad (293)$$

One can approximate the transformed values of f with the function S_F as close as possible by taking F large enough. Yet the $|C\sin Fr|$ function may be made arbitrarily large and

$$\bar{f}(r) = f(r) + C\sin Fr \qquad (294)$$

will transform as f(r) with little to no resemblance to f(r) for large values of C. Therefore, one can generate transforms that come as close to the desired values, g(x), within any desired accuracy as one may wish and still have no idea what the accuracy with respect to f(r) may be.

The technique used to remove this instability is to require the addition of a constraining relation on f(r) other than equation (290). This may be done either explicitly or implicitly. The proper relation must contain the desired qualities of f(r) requiring a high degree of a priori knowledge. Out of the near-infinite set of possible solutions for f(r) generated by the inversion, the constraining relation will act as a filter to obtain the unique, or near-unique, solution.

The presence of measurement error in the $g(x_i)$, larger than some quadrature error, allows the use of an appropriate quadrature approximation of the form:

$$\int_a^b h(y)\,dy \simeq \sum_{j=1}^{K} w_j h(y_j)\,\Delta y_j \qquad (295)$$

for k intervals of the argument y and the w_j are the quadrature weighting coefficients with increments Δy_j. For equation (290):

$$g(x_i) = \sum_{j=1}^{k} w_{ij} K(x_i, r_j) f(r_j) \Delta r_j \qquad (296)$$

where i represents a measurement and j a radii interval.

Define; for n measurements:

1. column vector G: $g_i = g(x_i) \quad i = 1, \ldots, n;$ (297)
2. coefficient matrix A: $a_{ij} = w_{ij} K(x_i, r_j)$ (298)
   $j = 1, \ldots, k;$ k radii intervals
3. column vector N: $N_j = f(r_j)\, \Delta r_j$ (299)

Then, equation (296) may be written as a matrix multiplication:

$$G = AN \qquad (300)$$

The value N_j represents the total number of particles per unit volume with radii between r_j and $r_j + \Delta r_j$, as can be seen via (288):

$$N_j \simeq \int_{r_j}^{r_j+\Delta r_j} f(r)\, \partial r = f(r_j)\left[(r_j + \Delta r_j) - r_j\right] \qquad (301)$$

and $f(r_j)$ is considered constant over the interval j. It is further assumed that the scattering functions have only small variations within each sub-interval radii range.

The problem has now been reduced to solving for the k unknowns in N given the (k)x(n) computed values in A and the n measurements in G. It must be emphasized that a quadrature approximation will introduce serious error in f(r) unless the quadrature weighting formula is of an accuracy higher than that of the expected measurement error. Let n_0 be the number of independent observations made such that $n_0 \leq n$. If $k = n_0$, then N may be solved for exactly:

(require A to be non-singular)

$$\Rightarrow \quad A^{-1}A = AA^{-1} = 1 \qquad (302)$$

where: 1 in a matrix equation represents the identity matrix,

$$(300): \quad AN = G \Rightarrow \hat{N} = A^{-1}G, \quad (k = n_0) \qquad (303)$$

where $\hat{N}$ represents the interpolated solution vector. However, if k $< n_0$, then N may be solved by minimizing the square of the error (least-squares):

(require A^TA be non-singular $\Rightarrow$ A^T: transpose of A)

(300): $$(A^TA)N = A^TG \qquad (304)$$

this step forms a square matrix which may be inverted,

$$\hat{N} = (A^TA)^{-1}A^TG \quad , \quad (k \leq n_0) \qquad (305)$$

That this last equation actually minimizes the error may be visualized by considering an appropriate spatial geometry which contains the vector G and the vector AN_1 where $N_1 \neq N$. See figure 10. The vector $G-AN_1$ is seen to be representative of the error vector between G and AN_1. The minimum error occurs when this error vector has the smallest magnitude, thus:

$$(AN_1)\cdot(G-AN_1) = 0 \qquad (306)$$

(the • represents the vector dot product).

Then for any $A\hat{N}$ in the range of A, the vector AN_1 is still perpendicular to it:

$$(AN_1)\cdot(G-A\hat{N}) = 0 \qquad (307)$$

Writing the dot product as a matrix multiplication requires:

$$(AN_1)^T(G-A\hat{N}) = 0 \qquad (308)$$

$$\Rightarrow N_1^T(A^TG-A^TA\hat{N}) = 0 \qquad (309)$$

And $N_1^T \neq 0$ since it represents any N_1 vector in the range, thus:

(304) $$A^TA\hat{N} = A^TG$$

In the work that follows, when writing the inverse matrix A^{-1}, if the matrix is not square, the quantity $(A^TA)^{-1}A^T$ is implied.

The procedure as indicated by equations (303) and (305) are in large

n-Space vector geometry

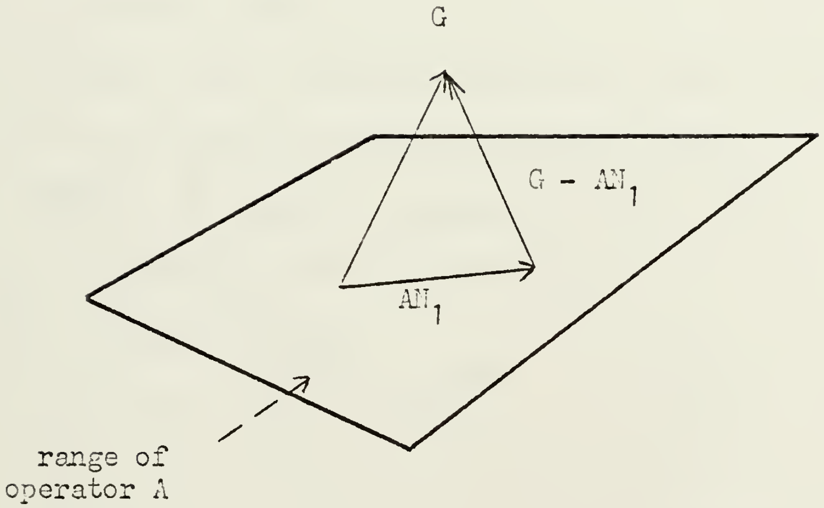

Figure 10

unsuccessful as they do not contain the constraining criterion. Some further problems concern the size of k.

1. Small k: the vector $\hat{N}$ does not accurately represent N due to the r_j set sparsity and/or the crudeness of the quadrature.

2. Large k: the components of $\hat{N}$ take on an oscillatory behaviour irrespective of N and the coefficients in A become particularly sensitive to round off error.

This sensitivity in coefficients is best characterized by the condition number of A (or any matrix) [5]:

$$\mathrm{cond}(A) = |A|\,|A^{-1}| \tag{310}$$

where $|A|$ - norm of a matrix

The norm of a matrix may be defined in any one of three ways depending upon the desire of the user to highlight specific aspects:

$$|A|_1 = \max_{1 \le j \le K} \sum_{i=1}^{n} |a_{ij}| \quad : \text{maximum column-sum} \tag{311}$$

where $|a_{ij}|$ - magnitude of the component a_{ij}

$$|A|_\infty = \max_{1 \le i \le n} \sum_{j=1}^{K} |a_{ij}| \quad : \text{maximum row-sum} \tag{312}$$

(normally used) $$|A|_e = \left(\sum_{i=1}^{n} \sum_{j=1}^{K} |a_{ij}|^2 \right)^{1/2} \quad : \text{Euclidean norm} \tag{313}$$

Because A^{-1} must be computed and will contain at least the inaccuracies in A, the cond(A) will be costly to compute and inaccurate as well. However, the test is the magnitude of the cond(A). If large, the matrix A is termed poorly-conditioned and the likelihood of a successful inversion decreases rapidly to zero. Corrections, like scaling or partial pivoting, must then be applied to A. Note, for the identity matrix, cond(1) = 1;

$$\mathrm{cond}(A) \geq 1 \tag{314}$$

since A^{-1} must exist. Other properties of the norm are:

$$|A| \geq 0 \qquad (315)$$

$$|A| = 0 \text{ iff } A = 0 \qquad (316)$$

$$|\beta A| = \beta |A|, \ \beta > 0 \text{ and a number} \qquad (317)$$

$$|A + B| \leq |A| + |B| \qquad (318)$$

$$|BA| \leq |B|\,|A| \qquad (319)$$

The cond(A) is most useful in bounding the error expected in the computed solution and relating this error to the magnitude of the residuals.

Define:

$$AX = B \qquad (320)$$

where X - exact solution vector

$\hat{X}$ - approximate solution vector

B - vector of known quantities

A - operator matrix

The residuals are:

$$R = B - A\hat{X} \qquad (321)$$

where R - residual vector

and:

$$E = X - \hat{X} \qquad (322)$$

Then:

$$R = AE \qquad (323)$$

Using E by inverting equation (323) and the norm relations (315)-(319), one may incorporate the cond(A) as an error measure:

$$\frac{1}{\mathrm{COND}(A)} \frac{|R|}{|B|} \leq \frac{|E|}{|X|} \leq \mathrm{COND}(A) \frac{|R|}{|B|} \qquad (324)$$

Therefore, the relative error in $\hat{X}$, contained in E, can be as great as the relative residual times the cond(A) and as small as this same residual divided by cond(A). For large cond(A), the residual yields little to no information on the accuracy in $\hat{X}$. Equations (320)-(323) may be used to define an iterative improvement algorithm (IIA).

1. compute $\hat{X}$ by $\hat{X} = A^{-1}B$ (325)

(321) 2. compute R by $R = B - A\hat{X}$

3. compute $\hat{E}$ by $\hat{E} = A^{-1}R$ (326)

4. correct X by $X \cong \hat{E} + \hat{X}$ (327)

If the system matrix A has errors in its coefficients, the system may then become ill-conditioned even if the residuals are small.

$$\hat{A} = A + H \tag{328}$$

where A - true coefficients

H - error in coefficients

The equation actually being solved is:

$$\hat{A}\hat{X} = B \tag{329}$$

Then, analogous to (324):

$$\frac{|X - \hat{X}|}{|\hat{X}|} \leq \text{COND}(A) \frac{|H|}{|A|} \tag{330}$$

The relative error in the residual can then be no larger than the relative error in the coefficients in A times the cond(A).

Finally, an approximate accuracy check may be obtained from [5]:

$$\text{if} \quad \frac{|E \text{ or } H|}{|\hat{X}|} \sim 10^{-P}, \tag{331}$$

then $\hat{X}$ is probably correct to p digits.

Equation (300) is assumed to be accurate within a small measurement error and equations (303) and (305) are considered insufficient to remove the inversion instability. There are several techniques available to remove thses instabilities of which three will be briefly covered.

The first method attempts to smooth the instabilities by one of two means. Define:

$$u(N) = (G - AN)^T(G - AN) + \gamma_1 (N - N_0)^T(N - N_0) + \gamma_2 (BN)^T(BN) \tag{332}$$

where $u(N)$ - the smoothing measure (a number)

$\gamma_1, \gamma_2 > 0$, numbers

N_0 - a priori information function, vector

B - matrix describing some desirable smoothing of N

$(G - AN)^T (G-AN)$ - a measure of the accuracy with which N satisfies equation (300)

$(N - N_0)^T (N - N_0)$ - a measure of the departure of N from the expected N_0

$(BN)^T (BN)$ - a value that measures the departure of N from ideal smoothness ($BN = 0$)

The smoothing technique involves the minimizing of $u(N)$. Some matrix differentiation rules will be needed [19]:

$$\frac{\partial X^T X}{\partial X} = 2X \tag{333}$$

$$\frac{\partial AX}{\partial X^T} = A \tag{334}$$

$$\frac{\partial Y}{\partial X^T} = \frac{\partial Y}{\partial Z^T} \frac{\partial Z}{\partial X^T} \tag{335}$$

where X, Y, Z, are vectors and A is a matrix, all of the proper dimensions such that the indicated products are defined.

Condition 1: $\gamma_2 = 0$; requires a priori knowledge, N_0.

(332): $$u_1(N) = Y_0(N) + \gamma_1 Y_1(N) \tag{336}$$

where $$Y_0(N) = (G-AN)^T(G-AN) \tag{337}$$

$$Y_1(N) = (N-N_0)^T(N-N_0) \tag{338}$$

The required condition is:

$$u_1(N) = \text{minimum} \Rightarrow \frac{d}{dN} u_1(N) \Big|_{N=\hat{N}} = 0 \tag{339}$$

Utilizing (333)-(335); where 1 is the identity matrix:

$$\frac{dY_0}{dN} = -2A^T(G-AN) \tag{340}$$

$$\frac{dY_1}{dN} = 2 \cdot 1 (N-N_0) \tag{341}$$

Use (340) and (341) in (339):

$$\hat{N}_1 = (A^T A + \gamma_1 I)^{-1}(A^T G + \gamma_1 N_0) \tag{342}$$

This is the required solution to equation (300) given the constraint function N_0. Note that, by setting $\gamma_1 = 0$, one obtains equation (305). Since the multiplier, γ_1 , represents the difference magnitude between N_1 and N_0, one might expect to use the estimated error, (331), as a first guess at γ_1 .

Condition 2: $\gamma_1 = 0$; requires no pre-conceived solution.

(332): $$u_2(N) = Y_0(N) + \gamma_2 Y_2(N) \tag{343}$$

where Y_0 - as before (337)

$$Y_2(N) = (BN)^T(BN) \tag{344}$$

The most common selection for B requires the solution to be smooth through the second derivative. In difference equation form:

$$N_j = N(r_j) \tag{345}$$

$$N_j' = \frac{dN_j}{dr} \simeq \frac{\Delta N_j}{\Delta r_j} = \frac{N_{j+1} - N_j}{r_{j+1} - r_j} = N_j' \tag{346}$$

$$N_j'' = \frac{dN_j'}{dr} \simeq \frac{\Delta N_j'}{\Delta r_j} = \frac{N_{j+1}' - N_j'}{r_{j+1} - r_j} = \frac{1}{\Delta r_j}\left(\frac{N_{j+2} - N_{j+1}}{\Delta r_{j+1}} - \frac{N_{j+1} - N_j}{\Delta r_j}\right) \tag{347}$$

Assume equally spaced quadrature points:

$$r_j = r_1 + (j-1)\frac{(r_2 - r_1)}{(K-1)} \tag{348}$$

$$\Delta r_j = r_{j+1} - r_j = \frac{r_2 - r_1}{K-1} = \Delta r \tag{349}$$

Note that Δr_j is independent of j. Thus:

$$N_j'' = \frac{1}{\Delta r^2}\left(N_j - 2N_{j+1} + N_{j+2}\right) \tag{350}$$

Since only the coefficients of N_j are important, ignore the $1/\Delta r^2$ scale factor and write:

$$N_j'' = \begin{pmatrix} 1 & -2 & 1 \end{pmatrix} \begin{pmatrix} N_j \\ N_{j+1} \\ N_{j+2} \end{pmatrix} \tag{351}$$

or $$N'' - BN \qquad (352)$$

in matrix form where B is a (k)x(k) matrix defined as:

$$B = \begin{pmatrix} 1 & -2 & 1 & 0 & \dots & 0 & 0 & 0 \\ 0 & 1 & -2 & 1 & \dots & 0 & 0 & 0 \\ 0 & 0 & 1 & -2 & \dots & 0 & 0 & 0 \\ 0 & 0 & 0 & 1 & \dots & 0 & 0 & 0 \\ \cdot & \cdot & \cdot & \cdot & & \cdot & \cdot & \cdot \\ \cdot & \cdot & \cdot & \cdot & & \cdot & \cdot & \cdot \\ \cdot & \cdot & \cdot & \cdot & & \cdot & \cdot & \cdot \\ 0 & 0 & 0 & 0 & \dots & 1 & -2 & 1 \\ 0 & 0 & 0 & 0 & \dots & 0 & 1 & -2 \\ 0 & 0 & 0 & 0 & \dots & 0 & 0 & 1 \end{pmatrix} \qquad (353)$$

The vector BN is thus the discrete analog of the second derivative of the unknown vector N. Other forms for B may be used, notably reference [20]. As before, the constraint shall be to minimize the quantity $u_2(N)$ in an effort to achieve the smoothest function N with a minimum of error in GN:

$$u_2(N) = \text{minimum} \Rightarrow \frac{d}{dN} u_2(N) \Big|_{N=\hat{N}} = 0 \qquad (354)$$

and $$\frac{d}{dN} Y_2 = 2B^T BN \qquad (355)$$

Now, (340) and (355) in (354):

$$\hat{N}_2 = (A^T A + \gamma_2 B^T B)^{-1} A^T G \qquad (356)$$

This is the required solution to (300) which satisfies the constraints outlined above. Again, setting $\gamma_2 = 0$ yields (305). A recent work into this particular solution has yielded considerations for the choice of γ_2. [20] If the factor γ_2 is too small, the instabilities are not removed from the final solution. And if chosen too large, the system becomes overconstrained and independent of the measurements. The best

choice appears to be $\gamma_2 \sim 10^{-4}$ and should be so chosen until further efforts provide a better choice.

Both solutions via this technique and the results from the next method may be improved in the iterative fashion as outlined in equations (321), (325)-(327); IIA. The algorithm:

(initial estimate) 1. obtain $\hat{N}^{(1)}$ by (342), (356), or (366)

(m^{th} residual) 2. $R^{(m)} - G - A\hat{N}^{(m)}$ (357)

(m^{th} error estimate) 3. $AE^{(m)} = R^{(m)} \Rightarrow \hat{E}^{(m)} = A^{-1}R^{(m)}$ (358)

(new estimate) 4. $\hat{N}^{(m+1)} = \hat{E}^{(m)} + \hat{N}^{(m)}$ (359)

(test) 5. is $|R^{(m)}| <$ some small positive number δ ?

no: $m = m + 1$, go to step 2.

yes: done, the solution is $\hat{N}^{(m+1)}$ to an accuracy on the order of δ.

The next method involves the computation of some statistical parameters. Only the general outline shall be described. See reference [21] for details. Let Γ_1 and Γ_2 be positive definite matrices (all eigenvalues positive) that act as weighting functions, then:

$$v(N) = (G - AN)^T \Gamma_1 (G - AN) + (N - N_0) + \Gamma_2 (N - N_0) \tag{360}$$

where Γ_1 is (n)x(n) and Γ_2 is (k)x(k).

Let N_0 be the mean vector for N as compiled from previous statistical data (model). Define the expected value operator E as:

$$E\left[g(x)\right] = \lim_{n \to \infty} \sum_{i=1}^{n} g(x_i) f(x_i) \tag{361}$$

where f(x) is the probability density function for g(x). Let the vector ε have zero mean and measure the error in G. Define the covariance matrices thus:

$$S_N = E\left[(N - EN)(N - EN)^T\right] \tag{362}$$

$$S_\varepsilon = E\left[\varepsilon\varepsilon^T\right] \tag{363}$$

Assuming a normal distribution for ε and N, then the Gauss-Markov theorem yields a statistically optimum estimate $\hat{N}_s$ by minimizing v(N) for:

$$\Gamma_1 = S_\varepsilon^{-1} \tag{364}$$

$$\Gamma_2 = S_N^{-1} \tag{365}$$

then: $$\hat{N}_s = X^{-1}A^T S_\varepsilon^{-1}(G - AN_0) + N_0 \tag{366}$$

where $$X = S_N^{-1} + A^T S_\varepsilon^{-1} A \tag{367}$$

The resulting covariance matrix for $(N - \hat{N}_s)$ is found to be X^{-1}. Thus, the expected mean square error may be written as:

$$E\left[(N-\hat{N}_s)^T(N-\hat{N}_s)\right] = \text{trace } X^{-1} \tag{368}$$

Without solving equation (300), one can thus obtain an accuracy estimate for $\hat{N}_s$ under the stated statistical conditions. One can also apply the IIA, (357) - (359), to enhance the estimate $\hat{N}_s$.

The last technique to be considered is an iterative scheme somewhat analogous to the iterative improvement algorithm. The method used is the Landweber iteration.[14]. In general, an iterative guess, $N^{(0)}$ is made based on some a priori knowledge and then improved successively to form a sequence whose mth member, $N^{(m)}$, transforms to the measured G as m tends to infinite. The techniques' success is due to the automatic constraining of the oscillatory nature of $N^{(m)}$ for small m. This allows an approximation to G early enough to avoid the oscillations if the sequence is terminated when the residual error is on the order of the error in G. The Landweber algorithm uses:

$$\hat{N}_L^{(m)} = \hat{N}_L^{(m-1)} + A^T(G - A\hat{N}_L^{(m-1)}) \tag{369}$$

where $\hat{N}_L^{(0)}$ reflects the expected solution. If the coefficient matrix

has all positive components, the convergence will be improved by defining a diagonal matrix D:

$$D: \; d_{jj} = \left(\sum_{i=1}^{n} a_{ij} \right)^{-1} \qquad j = 1, \cdots, K \tag{370}$$

and rewriting the estimate as:

$$\hat{N}_o^{(m)} = \hat{N}_o^{(m-1)} + DA^T(G - A\hat{N}_o^{(m-1)}) \tag{371}$$

This completes this short survey of inversion techniques. A common feature for all of them is their use of a priori knowledge to constrain the selection of probable solutions in order to enhance the choice of the proper solution. Indeed, this criterion must be met by any technique the experimenter chooses for inversion, if he is to have any confidence in the results.

V. CONCLUSION

This paper has endeavored to present the requirements for a device designed to map the tropospheric aerosol properties on a real-time basis. The specific model equations were derived after a theoretical development was performed in such detail that the user became familiar with the limitations of the theory. A candidate for such a device that would utilize advantageously the specific theory characteristics is the laser radar, or LIDAR. The LIDAR system allows for the direct selection of the key paramaters of the theory and yields as output the required inputs for the data inversion to begin. A few inversion techniques were presented, but, due to the large available extent of such methods, the subject was by no means exhausted. The aerosol LIDAR must be capable of polarization measurements and fast wavelength scanning to increase the number of independent observations made. Such system capability

would decrease the required amount of a priori knowledge the experimenter must decide on.

Both present and future developments in fast processors and versatile lasers argue strongly for the design, construction, and use of a LIDAR aerosol analysis system.

APPENDIX: COMPUTATIONAL FORMULAE AND ALGORITHM

This section presents some further equations to facilitate the computation of the required fuctions from the Mie theory.

Backscatter: $\theta = 180^\circ$

$$\pi_n(180^\circ) = (-1)^{n+1}\,\frac{n}{2}\,(n+1) \tag{372}$$

$$\tau_n(180^\circ) = -\pi_n(180^\circ) \tag{373}$$

$$S_1(180^\circ) = \sum_{n=1}^{\infty}(-1)^n\left(n+\frac{1}{2}\right)(b_n-a_n) \tag{374}$$

$$S_2(180^\circ) = -S_1(180^\circ) \tag{375}$$

backscatter gain: $$G = Q_{sca}(180^\circ) = \frac{4}{\alpha^2}\left|\sum_{n=1}^{\infty}(-1)^n\left(n+\frac{1}{2}\right)(b_n-a_n)\right|^2 \tag{376}$$

Scattering functions:

recurrence relations:

$$\tau_n(\cos\theta) = \cos\theta\,\pi_n(\cos\theta) - \sin^2\theta\,\pi_n'(\cos\theta) \tag{377}$$

$$\pi_n(\cos\theta) = (\cos\theta)\left(\frac{2n-1}{n-1}\right)\pi_{n-1}(\cos\theta) - \left(\frac{n}{n-1}\right)\pi_{n-2}(\cos\theta) \tag{378}$$

$$\pi_n'(\cos\theta) = (2n-1)\,\pi_{n-1}(\cos\theta) + \pi_{n-2}'(\cos\theta) \tag{379}$$

$$\pi_0(\cos\theta) = 0 \tag{380}$$

$$\pi_1(\cos\theta) = 1 \tag{381}$$

$$\pi_0'(\cos\theta) = 0 \tag{382}$$

$$\pi_1'(\cos\theta) = 0 \tag{383}$$

Scattering coefficients: The equations for a_n and b_n may be written in terms of the logarithmic decrement function, $\eta_n(Z)$. The equations below have been so written and then incorporated into an algorithm that was used to compute the scattering and extinction efficiencies for a particular case of $m = 1.54(1-i0.001)$. These values were then plotted on the enclosed graphs to picture the oscillatory behaviour of the

scattering efficiency, Q_{sca}, for α from 0.1 to 17.0 in 0.1 increments. The data points were connected by straight line segments to complete the visualization. It must be realized that further structure may appear under finer resolution. The routine was programmed for the Hewlett-Packard model 41C machine with the program listing accompanying the figures.

$$Z = x + iy = Z_x + iZ_y \tag{384}$$

$$m = n_{opt}(1 - i\kappa) = m_x + im_y \tag{385}$$

$$\beta = m\alpha = \beta x + i\beta y \tag{386}$$

Note in the following that only $\eta'_n(\beta)$ requires a complex argument.

(186) $$Q_{ext}(\alpha) = \frac{2}{\alpha^2}\sum_{n=1}^{\infty}(2n+1)\,R_e(a_n+b_n)$$

(187) $$Q_{sca}(\alpha) = \frac{2}{\alpha^2}\sum_{n=1}^{\infty}(2n+1)\left\{|a_n|^2+|b_n|^2\right\}$$

$$a_n = \frac{\psi_n(\alpha)}{\zeta_n(\alpha)}\left[\frac{\eta_n^{(1)}(\beta) - m\,\eta_n^{(1)}(\alpha)}{\eta_n^{(1)}(\beta) - m\,\eta_n^{(3)}(\alpha)}\right] \tag{387}$$

$$b_n = \frac{\psi_n(\alpha)}{\zeta_n(\alpha)}\left[\frac{\eta_n^{(1)}(\alpha) - m\,\eta_n^{(1)}(\beta)}{\eta_n^{(3)}(\alpha) - m\,\eta_n^{(1)}(\beta)}\right] \tag{388}$$

$$\psi_0(\alpha) = \sin\alpha \tag{389}$$

$$\psi_1(\alpha) = \frac{\psi_0(\alpha)}{\alpha} - \chi_0(\alpha) \tag{390}$$

$$\psi_{n+1}(\alpha) = \frac{(2n+1)}{\alpha}\psi_n(\alpha) - \psi_{n-1}(\alpha) \tag{391}$$

$$\chi_0(\alpha) = \cos(\alpha) \tag{392}$$

$$\chi_1(\alpha) = \frac{\chi_0(\alpha)}{\alpha} + \psi_0(\alpha) \tag{393}$$

$$\chi_{n+1}(\alpha) = \frac{(2n+1)}{\alpha}\chi_n(\alpha) - \chi_{n-1}(\alpha) \tag{394}$$

(114) $$\zeta_n(\alpha) = \psi_n(\alpha) + i\,\chi_n(\alpha)$$

$$\psi'_n(\alpha) = \psi_{n-1}(\alpha) - \frac{(n+1)}{\alpha}\psi_n(\alpha) \tag{395}$$

$$\chi'_n(\alpha) = \chi_{n-1}(\alpha) - \frac{(n+1)}{\alpha}\chi_n(\alpha) \tag{396}$$

$$\zeta'_n(\alpha) = \psi'_n(\alpha) + i\,\chi'_n(\alpha) \tag{397}$$

$$\eta_n^{(3)}(\alpha) = \frac{\zeta'_n(\alpha)}{\zeta_n(\alpha)} \tag{398}$$

$$\eta_n^{(1)}(\alpha) = \frac{\psi'_n(\alpha)}{\psi_n(\alpha)} \tag{399}$$

$$\eta_n^{(1)}(\beta) = \frac{\beta[\beta + n\,\eta_{n-1}^{(1)}(\beta)] - n^2}{\beta[n - \beta\,\eta_{n-1}^{(1)}(\beta)]} \; ; \; \eta_0^{(1)}(\beta) = \frac{1}{\tan\beta} \qquad (400)$$

Algorithm

$$q_1(\alpha) = \sum_{n=1} (2n+1)\left\{|a_n(\alpha)|^2 + |b_n(\alpha)|^2\right\}$$

$$\Rightarrow Q_{sca}(\alpha) = \frac{2}{\alpha^2} q_1(\alpha)$$

$$q_2(\alpha) = \sum_{n=1} (2n+1)\,Re\left\{a_n(\alpha) + b_n(\alpha)\right\}$$

$$\Rightarrow Q_{ext}(\alpha) = \frac{2}{\alpha^2} q_2(\alpha)$$

```
Begin:  A.  1.  input:    $n_{opt}$ , $r$
            2.  compute:  $m_x$ , $m_y$
        B.  1.  input: $\alpha$, $\delta$ (required accuracy)
            2.  compute:  $\beta_x$ , $\beta_y$
            3.  assign:   $n=1$     $q_1(\alpha) = q_2(\alpha) = 0$
            4.  compute:  $\psi_0(\alpha)$ , $\psi_1(\alpha)$
                          $\chi_0(\alpha)$ , $\chi_1(\alpha)$
                          $\eta_0^{(1)}(\beta)$
        C.  1.  compute:  $\psi_n'(\alpha)$, $\chi_n'(\alpha)$
                          $\zeta_n(\alpha)$, $\zeta_n'(\alpha)$
                          $\eta_n^{(1)}(\alpha)$, $\eta_n^{(3)}(\alpha)$
            2.  compute:  $\eta_n^{(1)}(\beta)$     $a_n(\alpha)$, $b_n(\alpha)$
            3.  compute:  $q_1^{(n)}(\alpha) = q_1(\alpha) + (2n+1)\{|a_n(\alpha)|^2 + |b_n(\alpha)|^2\}$
                          $q_2^{(n)}(\alpha) = q_2(\alpha) + (2n+1)\,Re\{a_n(\alpha) + b_n(\alpha)\}$
            4.  test:  is  $\frac{|q_1^{(n)}(\alpha) - q_1(\alpha)|}{q_1^{(n)}(\alpha)} \geq \delta$ ?
                          yes:  go to D.1.
                          no:   go to C.5.
            5.  test:  is  $\frac{|q_2^{(n)}(\alpha) - q_2(\alpha)|}{q_2^{(n)}(\alpha)} \geq \delta$ ?
```

```
                      yes:  go to D.1.

                      no:   go to E.1.

D.  1.  assign:   $q_1(\alpha) = q_1^{(n)}(\alpha)$
                  $q_2(\alpha) = q_2^{(n)}(\alpha)$
    2.  compute:  $\psi_{n+1}(\alpha), \chi_{n+1}(\alpha)$
    3.  assign:   $\psi_{n-1}(\alpha) = \psi_n(\alpha)$
                  $\psi_n(\alpha) = \psi_{n+1}(\alpha)$
                  $\chi_{n-1}(\alpha) = \chi_n(\alpha)$
                  $\chi_n(\alpha) = \chi_{n+1}(\alpha)$
                  $\eta^{(1)}_{n-1}(\beta) = \eta^{(1)}_n(\beta)$
                  $n = n+1$

    4.  go to C.1.
E.  1.  compute:  $Q_{sca}(\alpha) = \left(\frac{2}{\alpha^2}\right) q_1^{(n)}(\alpha)$
                  $Q_{ext}(\alpha) = \left(\frac{2}{\alpha^2}\right) q_2^{(n)}(\alpha)$

    2.  output:   n(number of steps)
                  $Q_{sca}(\alpha)$
                  $Q_{ext}(\alpha)$

                                              Stop.
```

Scattering efficiency versus size parameter for sphere

$m = 1.54(1-i0.001)$

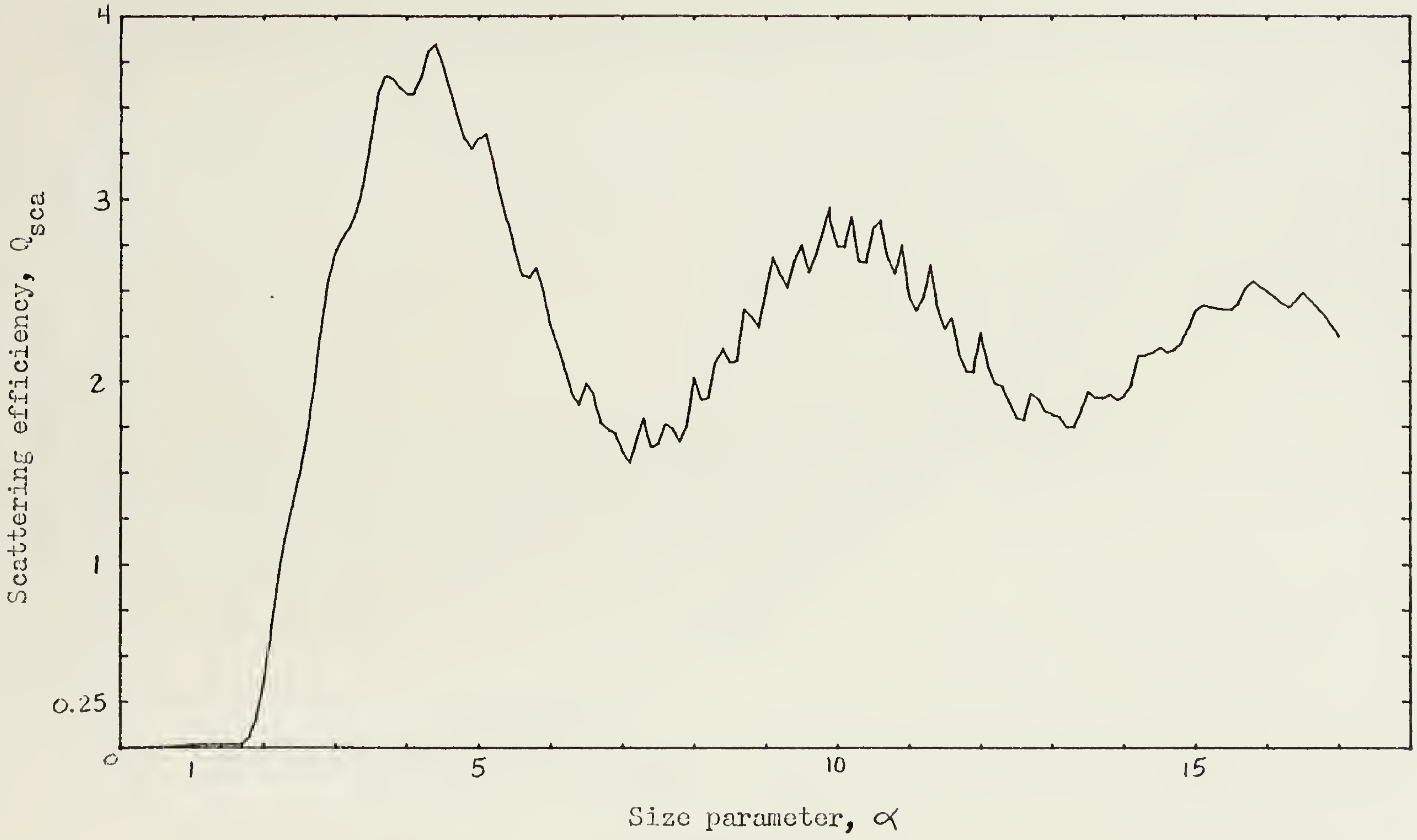

Figure 11

Scattering efficiency versus size parameter for shpere

$m = 1.54(1-i0.001)$

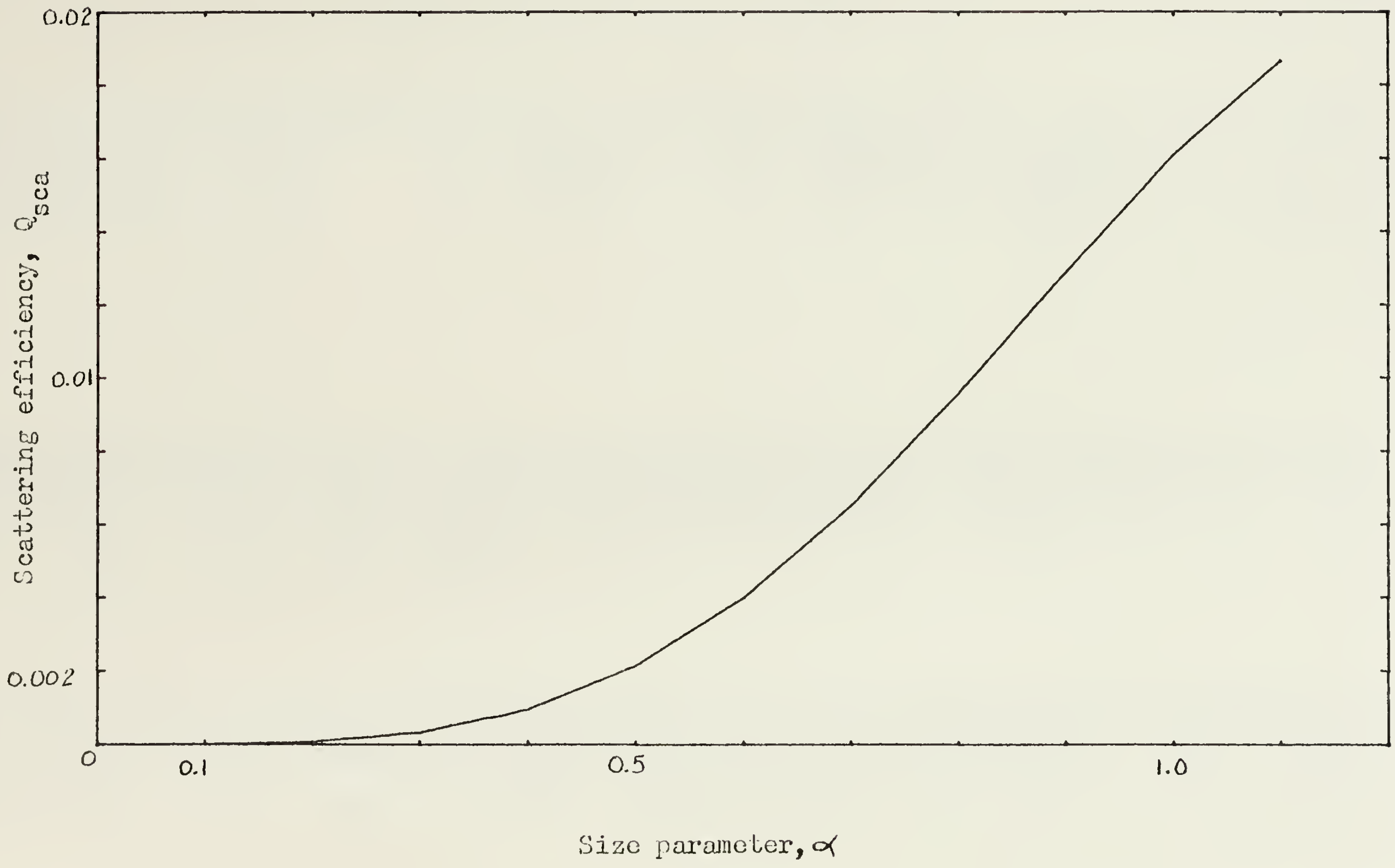

Figure 12

[illegible] (HP-41C) [illegible]

```
01◆LBL "MIE"
02 "INDEX ?"
03 PROMPT
04 STO 00
05 "RECIPR ?"
06 PROMPT
07 STO 01
08 RCL 00
09 *
10 CHS
11 STO 03
12 RCL 00
13 STO 02
14◆LBL 00
15 "ALPHA ?"
16 PROMPT
17 STO 04
18 CF 22
19 "ACCURACY ?"
20 PROMPT
21 FS? 22
22 GTO 01
23 1 E-3
24◆LBL 01
25 STO 05
26 RCL 04
27 RCL 02
28 *
29 STO 06
30 RCL 04
31 RCL 03
32 *
33 STO 07
34 0
35 STO 08
36 STO 09
37 1
38 STO 10
39 RCL 04
40 SIN
41 STO 11
42 RCL 04
43 COS
44 STO 13
45 RCL 11
46 RCL 04
47 /
48 RCL 13
49 -
50 STO 12
51 RCL 13
52 RCL 04
53
54 RCL 11
55 -
56 STO 14
57 RCL 07
58 RCL 06
59 XEQ "TNZ"
60 XEQ "1/Z"
61 STO 22
62 X<>Y
63 STO 23
64◆LBL 02
65 RCL 11
66 RCL 12
67 RCL 04
68
69 RCL 10
70 1
71 +
72 *
73 -
74 STO 17
75 RCL 13
76 RCL 14
77 RCL 04
78 /
79 RCL 10
80 1
81 +
82 *
83 -
84 STO 18
85 RCL 17
86 RCL 12
87 /
88 STO 19
89 RCL 18
90 RCL 17
91 RCL 14
92 RCL 12
93 XEQ "Z/"
94 STO 20
95 X<>Y
96 STO 21
97 RCL 23
98 RCL 10
99 *
100 RCL 22
101 RCL 10
102 *
103 RCL 07
104 RCL 06
105 XEQ "Z+"
106 RCL 07
107 RCL 06
108 XEQ "Z+"
109 RCL 10
110 X↑2
111 -
112 STO 32
113 X<>Y
114 STO 33
115 RCL 23
116 RCL 22
117 RCL 07
118 CHS
119 RCL 06
120 CHS
121 XEQ "Z*"
122 RCL 10
123 -
124 RCL 07
125 RCL 06
126 XEQ "Z*"
127 XEQ "1/Z"
128 RCL 33
129 RCL 32
130 XEQ "Z*"
131 STO 24
132 X<>Y
133 STO 25
134 RCL 03
135 RCL 19
136 CHS
137 *
138 RCL 02
139 RCL 19
140 CHS
141 *
142 RCL 25
143 RCL 24
144 XEQ "Z+"
145 RCL 14
146 RCL 12
147 XEQ "Z/"
148 RCL 12
149 +
150 STO 32
151 X<>Y
152 RCL 12
153 *
154 STO 33
155 RCL 21
156 RCL 20
157 RCL 03
158 CHS
159 RCL 02
160 CHS
161 XEQ "Z*"
162 RCL 25
163 RCL 24
164 XEQ "Z+"
165 XEQ "1/Z"
166 RCL 33
167 RCL 32
168 XEQ "Z*"
169 STO 26
170 X<>Y
171 STO 27
172 RCL 25
173 RCL 24
174 RCL 03
175 CHS
176 RCL 02
177 CHS
178 XEQ "Z*"
179 RCL 19
180 +
181 RCL 14
182 RCL 12
183 XEQ "Z/"
184 RCL 12
185 *
186 STO 32
187 X<>Y
188 RCL 12
189 *
190 STO 33
191 RCL 25
192 RCL 24
```

```
193 RCL 23
194 CHS
195 RCL 02
196 CHS
197 XEQ "Z+"
198 RCL 31
199 RCL 20
200 XEQ "Z+"
201 XEQ "1/Z"
202 RCL 33
203 RCL 32
204 XEQ "Z*"
205 STO 28
206 X<>Y
207 STO 29
208 X<>Y
209 R-P
210 X↑2
211 STO 32
212 RCL 27
213 RCL 26
214 R-P
215 X↑2
216 RCL 32
217 +
218 RCL 10
219 2
220 *
221 1
222 +
223 *
224 RCL 08
225 +
226 STO 30
227 RCL 28
228 RCL 26
229 +
230 RCL 10
231 2
232 *
233 1
234 +
235 *
236 RCL 09
237 +
238 STO 31
239 RCL 30
240 RCL 08
241 -
242 ABS
243 RCL 30
244 /
245 RCL 05
246 X<=Y?
247 GTO 03
248 RCL 31
249 RCL 09
250 -
251 ABS
252 RCL 31
253 /
254 RCL 05
255 X<=Y?
256 GTO 03
257 GTO 04
258•LBL 03
259 RCL 30
260 STO 08
261 RCL 31
262 STO 09
263 RCL 12
264 RCL 10
265 2
266 *
267 1
268 +
269 /
270 RCL 04
271 /
272 RCL 11
273 -
274 STO 15
275 RCL 12
276 STO 11
277 RCL 15
278 STO 12
279 RCL 14
280 RCL 10
281 2
282 *
283 1
284 +
285 *
286 RCL 04
287 /
288 RCL 13
289 -
290 STO 16
291 RCL 14
292 STO 13
293 RCL 16
294 STO 14
295 RCL 25
296 STO 23
297 RCL 24
298 STO 22
299 1
300 ST+ 10
301 GTO 01
302•LBL 04
303 2
304 RCL 04
305 X↑2
306 /
307 RCL 30
308 *
309 STO 34
310 2
311 RCL 04
312 X↑2
313 /
314 RCL 31
315 *
316 STO 35
317 BEEP
318 "STEPS = "
319 FIX 0
320 CF 29
321 ARCL 10
322 AVIEW
323 PSE
324 "CROSSECTIONS"
325 AVIEW
326 PSE
327 RCL 35
328 RCL 34
329 SF 29
330 FIX 7
331 "EXT="
332 ARCL Y
333 AVIEW
334 PSE
335 PSE
336 PSE
337 "SCA="
338 ARCL X
339 AVIEW
340 STOP
341 GTO 00
342•LBL "Z+"
343 X<>Y
344 RDN
345 +
346 RDN
347 +
348 R↑
349 RTN
350•LBL "1/Z"
351 R-P
352 X<>Y
353 CHS
354 X<>Y
355 1/X
356 P-R
357 RTN
358•LBL "Z*"
359 R-P
360 RDN
361 RDN
362 R-P
363 X<>Y
364 RDN
365 *
366 RDN
367 +
368 R↑
369 P-R
370 RTN
371•LBL "Z/"
372 XEQ "1/Z"
373 XEQ "Z*"
374 RTN
375•LBL "THZ"
376 2
377 *
378 STO 36
379 COS
380 X<>Y
381 2
382 *
383 STO 37
384 CHS
385 E↑X
386 RCL 37
387 E↑X
388 +
389 2
390 /
391 +
392 STO 38
393 RCL 37
394 E↑X
395 RCL 37
396 CHS
397 E↑X
398 -
399 2
400 /
401 RCL 38
402 /
403 RCL 36
404 SIN
405 RCL 38
406 /
407 RTN
408 END
```

LIST OF REFERENCES

1. Arfken, G., Mathematical Methods for Physicists, 2d. ed., Academic Press, 1970.

2. Caputo, B., Leonard, D.D., and Guagliardo, J., "LIDAR for Hire," Optical Spectra, 14, pp. 57 - 62, 1980.

3. Daily, J.W. and Harleman, D.R.F., Fluid Dynamics, 2d. ed., Addison Wesley, 1973.

4. Deirmendjian, D., Electromagnetic Scattering on Spherical Polydispersions, Elsevier, 1969.

5. Gerald, C.F., Applied Numerical Analysis, 2d. ed., Addison Wesley, 1978.

6. Grossman, R.L., "The Atmospheric Environment," in Remote Sensing of the Troposphere, ed. by V.E. Derr, University of Colorado, 1972.

7. Hall, F.F., Jr., and Ageno, H.Y., "Absolute Calibration of a Laser System for Atmospheric Probing", Applied Optics, 9, pp. 1820 - 1824, 1970.

8. Hecht, E. and Zajac, A., Optics, 3d. ed., Addison Wesley, 1976.

9. Hoel, P.G., Introduction to Mathematical Statistics, 4th ed., Wiley, 1971.

10. Ishimaru, A., Wave Propagation and Scattering in Random Media, 2 vols., Academic Press, 1978.

11. Junge, C.E., Air Chemistry and Radioactivity, Academic Press, 1963.

12. Kerker, M., The Scattering of Light and Other Electromagnetic Radiation, Academic Press, 1969.

13. Kolman, B., Introductory Linear Algebra, Macmillian, 1976.

14. Landweber, L., "An Iteration Formula for Fredholm Integral Equations of the First Kind," American Journal of Mathematics, 73, pp. 615-624, 1951.

15. Ott, R.H., "Scattering, Propagation, and Refraction of Electromagnetic and Acoustic Waves," in Remote Sensing of the Troposphere, ed. V.E. Derr, University of Colorado, 1972.

16. Panofsky, W.K.H. and Phillips, M., *Classical Electricity and Magnetism*, 2d. ed., Addison Wesley, 1962.

17. Schwarz, W.M., *Intermediate Electromagnetic Theory*, Wiley, 1964.

18. Schwiesow, R.L., "Atomic, Molecular, Particulate, and Collective Generalized Scattering," in *Remote Sensing of the Troposphere*, ed. by V.E. Derr, University of Colorado, 1972.

19. Selby, S.M., *Standard Mathematical Tables*, 17th ed., Chemical Rubber Company, 1969.

20. Shaw, G.E., "Inversion of Optical Scattering and Spectral Extinction Measurements to Recover Aerosol Size Spectra," *Applied Optics*, 18, pp. 988 - 993, 1979.

21. Strand, O.N. and Westwater, E.R., "Minimum RMS Estimation of the Numerical Solution of a Fredholm Equation of the First Kind," *S.I.A.M. Journal of Numerical Analysis*, 5, pp. 287 - 295, 1968.

22. Strand, O.N. and Westwater, E.R., "Inversion Techniques," in *Remote Sensing of the Troposphere*, ed. by V.E. Derr, University of Colorado, 1972.

23. Strauch, R.G. and Cohen, A., "Atmospheric Remote Sensing with Laser Radar," in *Remote Sensing of the Troposphere*, ed. by V.E. Derr, University of Colorado, 1972.

24. Van de Hulst, H.C., *Light Scattering by Small Particles*, Wiley, 1957.

INITIAL DISTRIBUTION LIST

		Copies
1.	Defense Technical Information Center Cameron Station Alexandria, Virginia 22314	2
2.	Library, Code 0142 Naval Postgraduate School Monterey, California 93940	2
3.	Department Chairman, Code 61 Department of Physics and Chemistry Naval Postgraduate School Monterey, California 93940	2
4.	Professor E. C. Crittenden, Jr., Code 61 Ct (thesis advisor) Department of Physics and Chemistry Naval Postgraduate School Monterey, California 93940	2
5.	LT Dale Robert Hamon, USN (student) 5850 S.W. 14th Street Miami, Florida 33144	2

Thesis 189505
H1758 Hamon
c.1 An analysis of LIDAR
atmospheric remote
sensing.

thesH1758
An analysis of LIDAR atmospheric remote
3 2768 002 07600 2
DUDLEY KNOX LIBRARY